conbots
CONnected through roBOTS

Deliverable D4.3

Preliminary experiments on learning with/out physical communication

This project has received funding from the European Union's Horizon 2020 research and innovation programme under grant agreement N. 871803

WP4 – Control of physical interaction and Game Theory of haptic communication

TASK 4.2 – Physical communication and motor learning

D4.3 – Preliminary experiments on learning with/out physical communication

Contract number:	871803
Project acronym:	CONBOTS
Project title:	CONnected through roBOTS: physically coupling humans to boost handwriting and music learning
Planned delivery date:	June 30th, 2022 (M30)
Author(s):	Etienne Burdet, Ekaterina Ivanova, Alessia Noccaro, Xiaoxiao Cheng, Jonathan Eden and Domenico Formica
Partners contributed:	ICL, UCBM
Document date:	07/07/2022
Version:	3
Revision:	0
Deliverable type:	Report
Abstract:	This deliverable describes a set of studies which extend previous studies on haptic communication by investigating: (i) the learning resulting from haptic communication; (ii) the underlying adaptation of muscle activation in interacting partners; (iii) 3D tracking against gravity and with asymmetric connections. It resumes the experimental protocols, the setup and the results of three studies carried out at ICL and UCBM.
Status:	☒ PU (Public) ☐ PP Restricted to other programme participants (including the Commission Services) ☐ Restricted to a group specified by the consortium (including the Commission Services) (please specify the group) ☐ Confidential, only for members of the consortium (including the Commission Services)

This project has received funding from the European Union's Horizon 2020 research and innovation programme under grant agreement N. 871803

The content of this deliverable does not reflect the official opinion of the European Union. Responsibility for the information and views expressed therein lies entirely with the author(s)

Document Revision Log

VERSION	REVISION	DATE	DESCRIPTION	AUTHOR
1	0	10/1/2022	Chapter 1	Ekaterina Ivanova
1	1	30/6/2022	Chapter 2	Xiaoxiao Cheng
1	2	30/6/2022	Summary	Etienne Burdet
1	3	30/6/2022	Chapter 3	Alessia Nocarro
2	0	5/7/2022	revision	Domenico Formica
2	1	6/7/2022	editing	Etienne Burdet
3	0	7/7/2022	Final version	Domenico Formica

Contents

Executive Summary

Recent studies have shown that when human subjects are connected by a (virtual) spring during the tracking of a randomly moving target, their tracking error decreases relative to solo performance [1, 2]. These benefits can be explained by the exchange of haptic information between connected subjects, that provides information on the target motion that complementing their vision [3, 4, 5]. This *haptic communication* between humans is critical to developing applications such as shared control or physical training. The present deliverable extends previous studies on haptic communication [1, 2, 3, 4, 5] by investigating: (i) the learning resulting from haptic communication, (ii) the underlying adaptation of muscle activation in interacting partners, and (iii) if asymmetric stiffness between partners can be used to improve performance.

Learning with/out haptic communication While subject performance taken directly after training has shown conflicting results on the effect of haptic communication [1, 2], to our knowledge no study has evaluated the retention of this learning that will determine its long term effect. In this context, Chapter 1 presents a study to compare the performance retention after training in characteristic conditions: without mechanical interaction, with trajectory guidance, or while interacting with a robotic or a human partner. The results show that while trajectory guidance yields the best performance during training, it dramatically reduces error variability and hinders learning. In contrast, the reactive human and robot partners do not impede the adaptation and allow the subjects to learn without modifying their movement patterns. Moreover, interaction with a human partner was the only condition that demonstrated an improvement in retention and transfer learning compared to a subject training alone. These results show the critical role that the exchange of haptic information has on efficient learning.

Body adaptation to improve haptic communication When helping my daughter to learn handwriting, is it better that I guide her with a

rigid hand, or that I relax my muscles to best feel where she wants to move? To address this question, Chapter 2 develops control modelling of the physical interaction between two agents during a tracking task. We analyse the interaction dynamics of the two agents considering the stochastic properties of their sensory signals, and how their combination depends on their mechanical impedance. Using stochastic nonlinear optimal control theory, we develop a strategy for improving the information exchange in interacting soft agents. The theoretical results are then systematically tested on a pair of connected robots and shown to improve the performance of human-robot interaction.

Using asymmetric mechanical connection to improve performance When mechanically connected individuals collaborate on a common task, both benefit from sharing haptic information [3], but their performance improvement relies on the more skilled partner increasing their effort to correct for inaccurate sensing [4]. When the partners are connected via two robotic interfaces, could these be used to amplify the force exerted on the less skilled partner and decrease the force the more skilled partner has to exert? Chapter 3 describes an experiment to test this hypothesis, where partners connected by a virtual elastic band with asymmetric elastic properties track a randomly moving target. The results first confirm previous results on haptic communication benefiting both interacting partners, on a more demanding task involving the control of position and orientation in 3D space with gravity and using commercial robots as interfaces. More importantly, they show that decreasing the connection rigidity on the side of the more skilled partner and decreasing it on the less skilled partner improves the tracking accuracy without requiring additional effort.

Chapter 1

Interaction with a reactive partner improves learning in contrast to passive guidance

Many tasks such as physical rehabilitation, vehicle co-piloting or surgical training, rely on physical assistance from a partner. While this assistance may be provided by a robotic interface, how to implement the necessary haptic support to help improve performance without impeding learning is unclear. In this paper, we study the influence of haptic interaction on the performance and learning of a shared tracking task. We compare in a tracking task the interaction with a human partner, the trajectory guidance traditionally used in training robots, and a robot partner yielding human-like interaction. While trajectory guidance resulted in the best performance during training, it dramatically reduced error variability and hindered learning. In contrast, the reactive human and robot partners did not impede the adaptation and allowed the subjects to learn without modifying their movement patterns. Moreover, interaction with a human partner was the only condition that demonstrated an improvement in retention and transfer learning compared to a subject training alone. These results suggest that for movement assistance and learning, algorithms that react to the user's motion and change their behaviour accordingly are better suited.

Introduction

Which shared control strategy can ensure good performance and learning to drive a semi-autonomous car or assist a child on their first bicycle ride? To guide the user's movement in robot-assisted applications, robotic interfaces traditionally use *trajectory guidance* (TG) with a spring-like force [6, 7, 8]. Such an interaction control strategy ensures accurate tracking of the reference trajectory, but can provide erroneous haptic information if the trajectory planned from the robot's sensors is not appropriate for the task. Training assisted by guidance considerably changes the learners' motion patterns by restricting movement freedom [9] and, therefore, can induce passive behaviour that can hinder the learning as well as its generalisation after the assistance is removed [10, 11, 12, 13, 14].

Could robot-assisted motor learning be improved by incorporating the strategies used by humans during shared control? Humans routinely interact with each other e.g. to carry large objects together or during dancing. Although during such joint tasks partners communicate only by the exchange of forces, they can swiftly coordinate motions and adjust their movements to the partner. Recent studies investigated such haptic interaction in pairs of subjects connected by an elastic band and carrying out a tracking task [1, 2], which revealed that *human partners* (HP) conspicuously exchange sensory information to improve their own performance [3, 4, 5]. The benefits of human-human interaction can be ascribed to the sensory sharing between connected partners enabled by the haptic channel. The *robotic partner* (RP) introduced in [3] to embody this haptic communication hypothesis was shown to provide similar performance and perception as human partners [9].

The benefits of interactive control with HP and RP suggest that it may be used to boost performance in collaborative tasks such as shared driving, rehabilitation training and joint object manipulation. However, it is still unclear whether learning with a human or robot partner would offer any advantage over training alone. The previous publications studying human-human interaction report conflicting results on the effect of this type of motion assistance on learning. Some studies [15, 1] have reported benefits of human-human interaction on learning, while in other studies no significant difference in performance was observed [16, 2], or it was found that learning strongly depends on the partners' skills during the interaction [17]. More importantly, these previous studies have only looked at the subject's performance change directly after the training session or at the differences within training, while sensorimotor performance can change with time [18], thus it is crucial to

assess motor performance after several days [19].

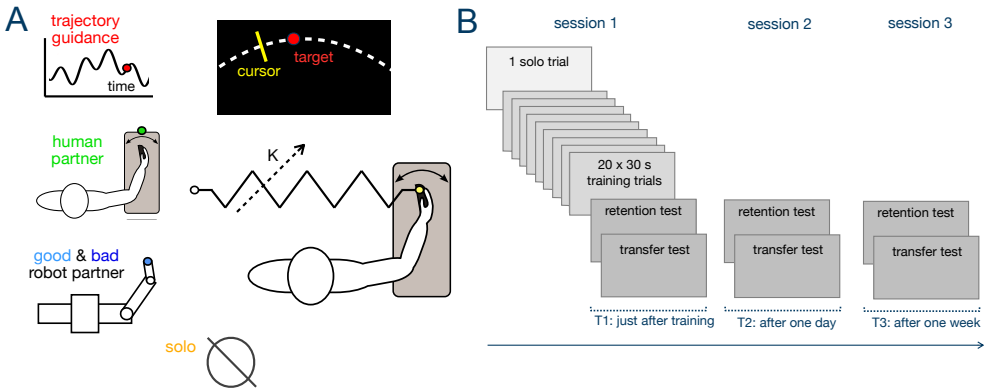

Figure 1.1: **Experiment description. A: Subjects use the Hi5 robotic interface to track a randomly moving target with their wrist flexion/extension. This occurs either without interaction (solo S) or while connected to: trajectory guidance (TG), their human partner (HP), or a reactive robot partner with less (RPg) or larger deviation (RPb). B: Experimental protocol with one solo performance test trial followed by 20 learning trials connected to one of the partners at the selected stiffness level. Performance after training was tested immediately after learning (T1), one day (T2) and one week (T3) later.**

Most studies of human assisted learning concern some type of trajectory guidance [20, 8, 21, 22, 14] where the results show that a learner usually relies on such assistance during the training, which results in reduced learning transfer when the connection with the assistance is removed. Only a few compliant or reactive robotic algorithms such as fading haptic guidance [14] and model predictive control [23] have been proposed and investigated in terms of learning. Moreover, the learning provided by robotic interaction control has been extensively investigated for reaching arm movements [24, 25, 26], which are carried out largely according to a predefined plan [27, 28]. For tracking tasks in which incoming sensory information must be continuously used, little research has considered the effects of robotic interaction.

We designed an experiment to analyse and compare the tracking performance, learning and retention that resulted from training with a human or the human-like robot partner controller of [3] relative to training with trajectory guidance or without interaction. Pairs of subjects, separated by a curtain preventing visual communication, moved their individual handle of the Hi5 dual robotic interface [29] to control a cursor on their own monitor (Fig.1.1A, 1.2A). Each subject was required to track a target moving along a

multi-sine function "as accurately as possible" using wrist flexion/extension of their dominant hand (see Methods). During the tracking task, subjects were connected to a partner agent by an elastic spring, where the partner angle would depend on their type.

Four interaction conditions were used in our experiments: *human partner* (HP), *"bad"* or *"good" robot partner* (RPb, RPg) with 40 % lower and 40 % higher accuracy than initial subjects' performance respectively, *trajectory guidance* (TG), as well as and three stiffness levels: *soft* (0.29 Nm/rad), *medium* (1.72 Nm/rad), *rigid* (17.02 Nm/rad), yielding twelve different experimental conditions, complemented by a *solo* condition (S) in which subjects performed the task without connection. 180 participants trained in one of these 13 conditions following the protocol of Fig. 1.1B. One familiarisation trial without interaction preceded 20 training trials with the specific human or robot partner and connection stiffness. Learning was assessed immediately after this training, one day later and one week later. Retention was evaluated in one trial with the same task as in the training, followed by one 30 s long trial with a different multisine target trajectory to test the transfer of learning (see Methods).

As interacting with a human partner will provide additional sensory information during interaction [3], our first hypothesis (H1) is that this will lead to better performance and learning than when training without interaction. We further assumed that the robot partner, based on such sharing of sensory information [3], will influence the learning in the same way as a human partner (H2). Finally, we anticipated from previous studies [13, 14] that trajectory guidance can impede learning when the interaction link is removed compared to training alone (H3).

Results

Impact of interactive control

We analysed the subjects' performance during the training phase while being connected to one of the interaction agents, as well as how the performance changed over the course of the training. In every partner and stiffness condition, the tracking error and error variability decreased from the first connected trial relative to the familiarisation trial that was performed solo (all $p<0.0001$) (Fig. 1.2B). Smoothness improved in the first

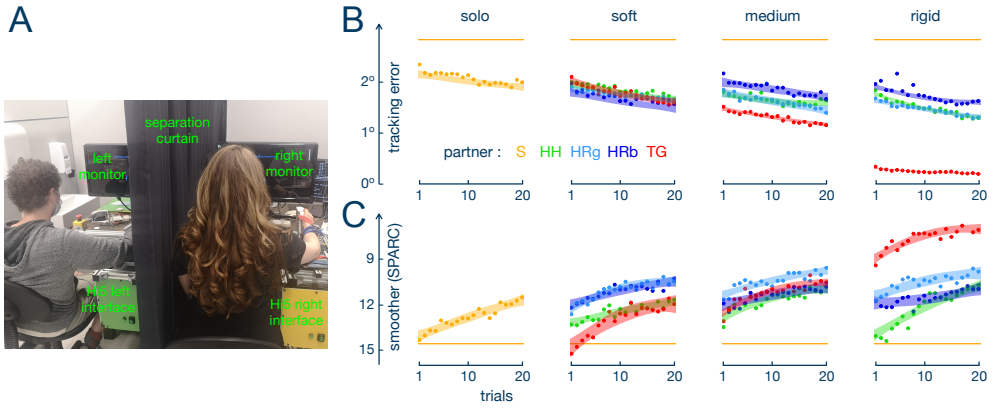

Figure 1.2: **A. Experimental setup for the tracking task: participants were separated by a curtain and tracked a visual target presented on the monitor using handles of the dual robotic interface Hi5. B. Learning analysis using the tracking error. C. Learning analysis using SPARC smoothness metric. The different connection conditions were: "solo" (no connection), "soft" 0.29 Nm/rad stiffness, "medium" 1.72 Nm/rad, "rigid" 17.02 Nm/rad. The dots represent the average of the corresponding metric for a trial and the area around it represents the ± 95% confidence interval estimated based on the least square fit of a second order polynomial. The horizontal yellow bars correspond to the metric's value in the initial trial.**

training trial when interacting with both the RPg and the RPb at every stiffness level (all $p<0.02$) (Fig. 1.2C). For the TG this strongly depended on the connection stiffness, where TG with the medium and rigid stiffness immediately increased smoothness ($t(308)=-2.533$, $p=0.028$ for the medium, $t(308)=-13.272$, $p<0.0001$ for the rigid connection), but no such effect was observed for the soft stiffness condition ($t(308)=0.106$, $p=0.980$). However, motion smoothness was not immediately improved while connected with a HP ($p>0.23$ for each stiffness values) or while conducting the task alone ($t(13)=8.568$, $p=0.325$).

The tracking error decreased in most conditions during the 20 training trials based on the difference between the first and the last five connected trials (all $p<0.05$) (Fig. 1.2A). One exception was the HP condition with medium stiffness, which did not improve the subjects' tracking accuracy during the training ($t(308)=2.036$, $p=0.073$). Another exception was the connection to TG with the rigid stiffness ($t(308)=2.036$, $p=0.299$), however, this condition resulted in a more accurate performance compared to the other groups from the first connected trial (all $p<0.0001$). Even though the accuracy in-

creased during the 20 connected trials, the error variability reduced in only some conditions: while connected to RPs at the medium stiffness (RPg: $t(308)=2.721$, $p=0.017$; RPb: $t(308)=2.323$, $p=0.048$), while working with TG at the soft and medium stiffnesses (soft: $t(308)=3.632$, $p=0.001$; medium: $t(308)=2.498$, $p=0.031$) and while completing the task with a HP at rigid stiffness ($t(308)=3.632$, $p<0.0001$). Learning was also indicated through a large increase of smoothness during the 20 trials for all partner and stiffness conditions including the solo condition (all $p<0.02$), except for the RPb group with medium ($t(308)=-1.952$, $p=0.1197$) and rigid stiffness ($t(308)=-1.568$, $p=0.221$) (Fig. 1.2B).

Adaptation to shared control

At the end of training, all groups exhibited similar error levels for the soft connection ($p>0.59$ for all pairwise comparisons for the averaged value over last five trials) (Fig. 1.3A). However, clear differences appeared for the other stiffness levels. For the medium connection, subjects from the TG group followed the target more accurately than the HP ($t(243)=-2.260$, $p=0.044$), RPb ($t(167)=-3.032$, $p=0.006$) and S ($t(167)=-5.306$, $p<0.0001$) groups. Furthermore, the RPg group showed less error than participants tracking the target solo ($t(167)=-3.247$, $p<0.014$). With the rigid connection, the TG resulted in a higher accuracy than all other conditions (all $p<0.0001$). Moreover, while rigidly connected, the HP and RPg conditions resulted in higher accuracy than conducting the task solo (S>HP: $t(167)=-4.371$, $p=0.0003$, S>RPg: $t(167)=-4.347$, $p=0.0003$).

As expected, the TG decreased the error dramatically with a stiffer connection: the error was lower with the medium stiffness compared to the soft connection ($t(308)=-2.254$, $p=0.044$) and with the rigid stiffness compared to less stiff connections (both $p<0.0001$). In contrast, the error was relatively insensitive to the connection stiffness in the RPg and RPb groups ($p>0.097$ for all pairwise comparisons between different stiffness levels for each group). Finally, the accuracy during the final trials with the HP was similar between the rigid and medium as well as between the soft and medium stiffness levels (both $p>0.2$). However, the accuracy was lower for the soft compared to the rigid connection ($t(308)=2.273$, $p=0.044$). The average error for the HP tends to be as low as with the RPg over all stiffness conditions ($t(154)=0.321$, $p=0.999$).

A similar pattern was observed for the error variability at the end of the

training: TG showed less variability than the HP ($t(266)=-2.721$, $p=0.017$), RPb ($t(266)=-2.843$, $p=0.013$) and S ($t(167)=-5.165$, $p<0.0001$) conditions with medium stiffness and less variability than all other conditions with rigid stiffness (all $p<0.0001$). Furthermore, the RPg resulted in less error variance than S with medium ($t(167)=-3.652$, $p=0.004$) and rigid ($t(167)=-4.477$, $p=0.0002$) connections. Interaction with a HP was only different from S for the rigid stiffness ($t(167)=-4.228$, $p=0.0004$). No differences between the partner conditions were found for the soft connection (all $p>0.24$), and the HP, RPg resulted in a similar variability for all connection levels ($t(154)=0.978$, $p=0.909$).

Roughly symmetric changes were observed for the last five trials on the smoothness (Fig. 1.3B). As expected, movements with the TG had the highest smoothness after training in the rigid condition compared to the other partner groups and solo condition ($p<0.0008$ for comparison with each partner condition for rigid stiffness level inclusive control group). Moreover, the smoothness for the TG was higher for the rigid stiffness than for the medium ($t(255)=4.372$, $p=0.0001$) and soft connections ($t(255)=6.050$, $p<0.0001$). Although in the first connected trial for the soft connection, movements with the TG were not particularly smooth relative to the RPs, at the end of the training no differences between these partner conditions were identified (all $p>0.13$). While at the beginning of the training with the rigid stiffness, interaction with another human resulted in the lowest smoothness among other condition, the differences between the HP and RPs disappeared after 20 trials (all $p>0.3$). No other differences between the groups were revealed for the last five connected trials (all $p>0.05$).

Acquired behaviour in visuomotor tracking

To evaluate the effect of learning on individual performance, we analysed the influence of the stiffness and partner conditions on the accuracy, error variability and smoothness in the retention and transfer trials. Figure 1.4A shows the tracking error using the training trajectory in the three retention trials – immediately after training, after one day and after one week. The analysis showed a significant effect of the partner condition on the retention accuracy ($F(3,153.45)=4.027$, $p=0.009$). We observed that training with the TG resulted in a larger error than training with a HP over all stiffness levels and trials ($t(154)=3.408$, $p=0.005$). A small difference was seen between TG and RPg groups, however, this comparison was not significant ($t(154)=2.317$, $p=0.065$). The tracking error for the TG with the rigid stiffness was also

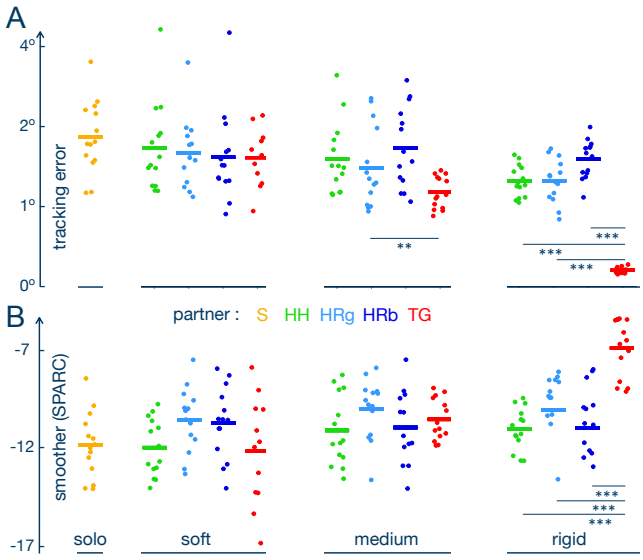

Figure 1.3: **Tracking performance and smoothness with the partner's assistance at the end of the training period. Each dot represents the average tracking error (A) and SPARC smoothness metrics (B) in the last five trials for one participant. The bars show the average value for each condition.**

larger relative to the S condition (t(167)=3.649, p=0.003) over all retention trials.

Error variability was also significantly impacted by the partner condition (F(3, 153.17)=5.377, p=0.0015). Subjects that trained with TG had significantly more variability in their retention trials than those with the HP (t(154)=3.950, p=0.0007) and then RPg (t(154)=2.508, p=0.0396) groups over all stiffness levels and retention trials. Moreover, the HP group showed less error variability in retention than S over all stiffness conditions (t(175)=-2.474, p=0.0377).

The retention smoothness did not change for different partner conditions (F(3, 154.34)=1.487, p=0.220), but was significantly influenced by the connection stiffness (F(2, 154.35)=3.176, p=0.045). Participants that trained solo had smoother movements in retention than those that trained with the rigid connection (t(176)=-2.287, p=0.047). The rigid stiffness also tended to have lower smoothness than the soft (t(154)=-2.059, p=0.062) and medium connections (t(154)=-2.282, p=0.062), however these results were not significant.

Clearer differences between the groups were observed along the independent trajectory used to infer the transfer of learning (Fig. 1.4B): the partner condition ($F(3, 153.53)=5.551$, $p=0.001$) as well as its interaction with the test time ($F(6, 299.10)=2.745$, $p=0.013$) had a significant effect on the tracking error in the transfer trial. In particular, the TG resulted in more error than all of the other groups after one week (HP<TG: $t(195)=-4.855$, $p<0.0001$; RPb<TG: $t(198)=-3.333$, $p=0.006$; PRg<TG: $t(198)=-4.016$, $p=0.0008$). Moreover, even immediately or one day after training the subjects that trained with the TG conducted their movements less accurately than those that trained with a HP (immediately: $t(194)=-2.883$, $p=0.016$; after one day: $t(198)=-3.063$, $p=0.011$) and than those in the RPg condition (immediately: $t(194)=-2.436$, $p=0.041$; after one day: $t(199)=-2.474$, $p=0.041$). The TG condition also had a larger error than the S condition for the rigid stiffness over all transfer trials $t(167)=3.291$, $p=0.011$). In contrast, the HP condition had a lower error than the S over all stiffness levels and retention trials ($t(175)=-2.475$, $p=0.037$).

The error variability in transfer was also influenced by the partner condition ($F(3, 152.24)=3.800$, $p=0.0116$) and its interaction with the test time ($F(6, 298.08)=2.8681$, $p=0.0099$). The differences in variability between partner conditions were observed only in the transfer trial after one week: TG showed more variability than the HP ($t(217)=4.199$, $p=0.0007$), RPb ($t(220)=3.135$, $p=0.0117$) and RPg conditions ($t(220)=3.673$, $p=0.0027$).

The transfer smoothness, similar to the retention smoothness, was influenced by the stiffness ($F(2, 154.32)=4.512$, $p=0.012$) and its interaction with trial ($F(4, 300.33)=3.216$, $p=0.013$). Training with the rigid connection resulted in lower smoothness than with the soft stiffness in the first retention trial ($t(227)=3.299$, $p=0.008$) and then with the medium stiffness after one day after training ($t(232)=3.152$, $p=0.008$).

Discussion

Our experiment investigated how subjects perform a tracking task with wrist flexion/extension on a relatively complex trajectory. This task demands continuous planing based on incoming sensory information, in contrast to the widely studied reaching arm movements that can be carried out largely according to an initial plan [27]. By comparing representative interactive controllers with regards to performance and learning, we analysed their ability to assist movement for shared control, and the tracking performance they

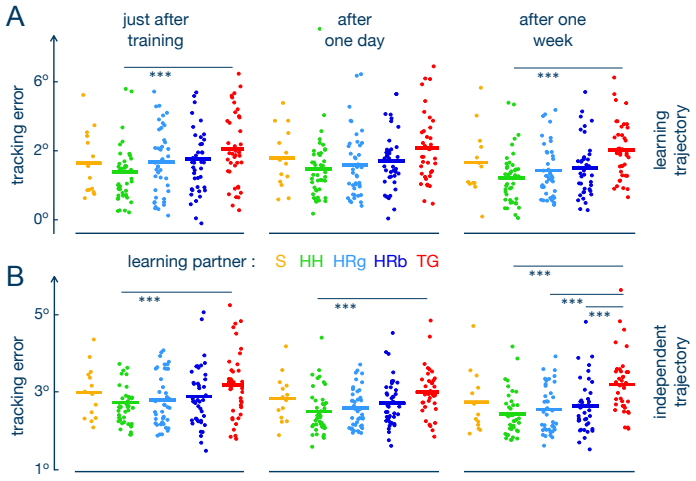

Figure 1.4: **Retention (A) and transfer (B) of the tracking performance without interaction after learning. Each dot represents the value of mean tracking error in the same trajectory used during training (A) and in an independent multisine trajectory (B). The bars show the average value for each condition.**

induce. This study is the first to analyze the long-term learning effect of training with a human partner (HP) and with the robotic partner (RP) of [3] up to one week of retention, compared to solo performance (S) and training with trajectory guidance (TG).

During the shared control stage, when the subjects were connected to one of the partner conditions, the TG, HP and RPg all reduced the tracking error significantly relatively to the S condition when the connection between the partners was rigid. However, the manner with which the TG does so is distinctively different to the HP and RP conditions. The TG uses an elastic force to the known desired trajectory and thus results in more accurate tracking with increased connection stiffness. This results in a nearly perfect accuracy from the first connected trial, dramatically decreases error variability, and leads to higher smoothness. As a consequence, assistance from TG induces a considerable change of motion patterns compared to what a learner would exhibit during solo training. In contrast, the HP and RP do not assume a-priori knowledge of the planed trajectory as they predict it [3]. The HP's or RP's movement is different from the target trajectory the tracking error relative to it and does not decrease with a more rigid connection and the motions characteristics are similar to the solo condition.

The effect of training with different interaction control modalities also sep-

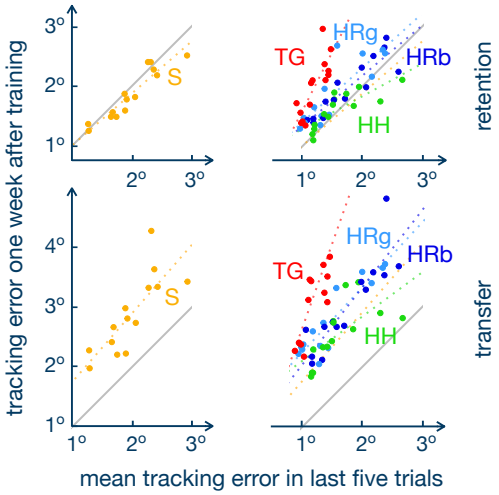

Figure 1.5: **Training tracking accuracy retension/transfer relationship. Accuracy is taken from the last five trials of training while the average performance in transfer and retention trials at medium stiffness is used. Dashed lines represent the least-square fit for each group. The grey line separates the graph so that in the upper triangle it contains participants with better performance just after training than one week later, while in the bottom triangle it has subjects who improved performance one week after training.**

arates the TG from the HP and RP as can be observed at the end of the training period, as is visualised in Fig. 1.5. The TG minimises the tracking error, error variability and smoothness while the connection is maintained. However, after it leads to deteriorating tracking performance as is particularly observed one week after training (Fig. 1.4B). This can also be observed from Fig. 1.5 where the TG had the stiffest slope in retention ($b=1.9639$, $t(12)=4.894$, $p=0.0004$) and in transfer ($b=2.8225$, $t(12)=3.542$, $p=0.0041$). Moreover, regression analysis revealed that the TG slope was different from all other groups in retention (all $p<0.027$) and from HP and RPg in transfer (both $p<0.45$). This observation confirms the H3 hypothesis and previous findings, where despite improved training performance during connection, haptic guidance impedes learning and its generalisation in path-following [30], continuous rhythmic [14] and timing-crucial [11] tasks as well as to control an unstable inverse pendulum [23].

Interestingly, the performance after training solo remains stable after one week (Fig. 1.4A), arguably corresponding to learned task performance. Similarly, performance after one week did not deteriorate further after training

with the RPs, where statistical comparison between the S and RP groups also did not exhibit a significant difference for the regression slopes. The HP, in contrast and in accordance with the H1 hypothesis, did show a tendency to improve after training relative to the S condition (Fig. 1.4B), which resulted in a more flat slope in Fig. 1.5 than other groups in retention (b=0.5457, t(12)=4.615, p=0.0006) and transfer (b=0.7387, t(12)=3.210, p=0.0076). These results might have been affected by the use of healthy subjects in a one-dimensional task and therefore need to be investigated further.

In this study we compared robot partners with high and low noise, which are different parameterisations of the RP, where the level of accuracy that the partner provides was varied. In this way we could test how the skill level of this human-like robot partner influenced learning. The RPg condition tended to lead to better performance during the training compared to the other conditions, however, after the training this effect disappeared and both RPs have a similar retention and transfer of the learned skills. The similarity of performance in retention and transfer regardless of the quality of the RP, suggests that for continuous tasks the accuracy of the robot partner might be not as important factor as the manner of how the partner interacts characterised by the intrinsic reactivity of the controller or its compliance. Since there is no difference between the robotic skill partner level and the learning with RPs is superior to TG, it is clear that assistance corresponding to the user's ongoing movement is preferable over assistance through trajectory guidance, which agrees with recent results comparing compliant predictive control with TG [23].

While tracking error and error variability are mostly influenced by the interaction modality during the training phase, motion smoothness in retention and transfer depended on the connection stiffness of the training partner. Regardless of the partner condition, training while connected through a rigid link impacted the smoothness negatively compared to training solo or with the soft and medium stiffness levels. This may be linked to the rigid stiffness reducing the subject's ability to freely move within the training, thereby not providing them with the opportunity to find more naturally smooth motions.

In summary, shared control with a human partner or the robotic partner of [3] leads to a reduction of the tracking error when moving together and increases the movement smoothness without impacting the ability to perform the task when alone or reducing some error variability in the motion. With the exception of working with a HP, no partner showed clear improvements in the retention or transfer trials compared to the S condition, where in particular TG resulted in reduced performance, which is likely due to slacking

[10, 12]. This may be explained with fundamentally different mechanisms of interaction: while TG physically guides the learner and restricts their own motion flexibility, HP and RP benefit performance and learning by providing additional sensory information. Due to TG modifying behaviour, e.g. by invoking passive performance, and its inability to deal with intrinsic human variability, TG is only suited to applications where the human cannot perform the task actively, as in robot-aided stroke rehabilitation for severely affected individuals. Instead, in applications such as active neurorehabilitation, shared driving [31] or co-pilot systems [32], an interaction with another human or RP is better suited. Furthermore, when learning is required, despite being widely used, the negative impact of TG on learning means again a HP or RP is more appropriate.

Finally, while the RPs generally exhibited similar behaviours to the HP condition during and after training, they present differences that are worth analysing. While a connection with RPs immediately improved the subjects' smoothness in the first training trial, interaction with a HP did not show this effect. Participants interacting with a HP also did not, in the medium stiffness condition, improve their accuracy during the training phase, while clear improvements were visible in all RPs conditions. Therefore, during the training the RPs showed a better performance than HP. It is however important to highlight that the HP was the only condition that showed a better accuracy than S in retention and transfer. This suggests that, contrary to the H2 hypothesis, there are unique characteristics of this human interaction that specifically possess the ability to improve motor learning. Identifying these characteristics and how to replicate them in human-like robot controllers as well as further generalisation of these results to robotic interfaces with higher degree-of-freedom and other tasks is therefore critical.

Conclusion

We evaluated human and human-like haptic interaction as mechanisms to improve motor learning in robot-assisted training, and compared these mechanisms to learning without a partner and using the trajectory guidance strategies commonly used in rehabilitation. Our observation of learning up to one week shows that trajectory guidance, which modifies the learner's behaviour considerably during interactive training, does not provide efficient learning. In contrast, both interaction with another human or with a human-like robot partner can result in improved learning and performance during interaction.

This suggests that human-like robot partners are a good mechanism for automated training, since they enable the exchange of sensory information without interfering/restricting the motion during interaction.

Methods

Participants

The experiment was granted ethical approval by the Research Ethics Committee of Imperial College London (reference 15IC2470). The study was performed in accordance with all relevant guidelines and regulations. 180 healthy volunteers (66 females and 134 males, aged 17-41 years with an average age of 24.2 and standard deviation of 3.8) took part in this study. Twelve participants were left-handed, 167 right-handed and one ambidextrous. 129 participants reported some experience with haptic devices such as gaming controllers or joysticks and 138 regularly play or used to play computer games (from 0.1 to 40 hours/week with a mean of 7.6 hours and standard deviation of 7.6 hours). 19 participants reported previous practice with a robotic interface.

Experiment setup and procedure

Before beginning all participants gave their informed consent to carry out the experiment, then filled in the Edinburgh handedness form [33] and a demographic questionnaire. They were instructed that within the experiment they might interact with a robot, another human, or complete the training without interaction. Subsequently, they were randomly assigned to one of the thirteen experimental groups. Altogether each group had 14 subjects, with the exception of the the TG group with the soft stiffness connection which had only 12 participants.

Subjects were seated in front of a monitor with their dominant hand connected to one of the handles of the Hi5 robotic interface. They used their hand to track the target trajectory shown on the screen, which was given (in degrees) by

$$q^*(t) \equiv 18.5 \, \sin\left(\frac{\pi \, t}{1.547}\right) \, \sin\left(\frac{\pi \, t}{2.875}\right) \, , \quad 0 \leq t \leq 30 \, s \, . \tag{1.1}$$

The interface yielded an elastic connection of the wrist flexion/extension $q(t)$

$$\tau(t) \equiv \kappa \left[q_r(t) - q(t) \right] \ Nm \,, \quad 0 \leq t \leq 30s \tag{1.2}$$

with the reference angle $q_r(t)$, which was differently set for each experimental condition, during 30 s long trials. The connection stiffness κ was set as one of $\{0.29,\ 1.72,\ 17.02\}$Nm/rad, since this parameter has been shown to impact the interaction behaviour as was detailed in [9]. The Hi5 was operated in torque control provided this interaction at 1000 Hz. Wrist angle data was simultaneously recorded at 100 Hz.

All subject pairs participated in three sessions as shown in Fig.1.1B. On the first day, they completed one test trial without any interaction torque, followed by with one of the interaction conditions for 20 30 s long trials with 10 s breaks in between. Learning was assessed immediately after training, after one day, and after one week. Each of these assessment consisted of one *retention trial* without interaction, followed by one *transfer trial* on a different trajectory given by

$$q^*(t) \equiv 22.2 \sin\!\left(\frac{\pi\,(t+1.2)}{1.547}\right) \sin\!\left(\frac{\pi\,(t+1.2)}{2.875}\right) , \quad 0 \leq t \ \leq \ 30\,s\,. \tag{1.3}$$

Experimental Conditions

The thirteen experimental groups corresponded to one control group that performed the complete experiment without working with a partner plus groups for each combination of partner agent {HP, TG, RPg, RPb} and stiffness level $\{0.29,\ 1.72,\ 17.02\}$Nm/rad. Each subject completed the training in only one of the thirteen condition (between-subjects study design).

For each different partner type the reference angle q_r was set differently. In the *trajectory guidance (TG)* condition, the subject performed the experiment connected to the reference trajectory such that $q_r = q^*$. The interaction force (1.2) therefore acted as a proportional position controller.

In the *human partner (HP)* condition, two subjects simultaneously performed the tracking with trajectory (2.14) by holding their respective robotic interface with a virtual spring connection between them, such that q_r was given by their partner's position. The subjects were not given explicit knowledge that they were working together but they were given indirect knowledge of their partners position through the interaction force (1.2).

Finally in the *good and bad robot partner (RPg and RPb)* conditions, the subjects were connected to a robot agent that tracked the measured target using the human-like partner algorithm of [3]. Here, the agent evolves q_r using a control input whh is given by the linear feedback control law

$$u = -L_p\big(q - \widehat{q^*}\big) + L_v\Big(\dot{q} - \widehat{\dot{q}^*}\Big)\,, \tag{1.4}$$

where L_p and L_v are the proportional and derivative gains and $\widehat{q^*}$ denotes the RP's target estimation. To obtain this target estimate, the RP combines its own measurement of the target with the partner's target estimated from the interaction force between them. This is achieved using a Kalman filter that uses the known dynamic model and a measurement consisting of both the partners own measurement and its estimation of the partner. The good and bad partners are achieved by altering the amount of noise in the RP's partner estimation. The RPb was set so that the resulting *tracking error*

$$\frac{1}{T}\int_0^T |\, q(t) - q^*(t)\,|\; dt\,, \quad T = 30s\,, \tag{1.5}$$

where q^* is the target position, of the partner had a 40% higher error compared to the subject's initial performance and the RPg was set to 40% lower error.

Statistical analysis

Performance and learning were analysed using the *tracking error* defined by eq.(2.12), the *error variability* defined as a characteristic of motion variability, calculated as a standard deviation of errors during each trial duration, as well as the *SPARC smoothness* metrics [34] that evaluates the complexity of the movement velocity $\dot{q}$. For all metrics the first 0.8 s of each trial was deleted to exclude the reaction time at the movement start and to analyse only the tracking performance. Metrics were analysed during the connection with a partner to estimate shared performance and after the link between partners was removed to evaluate the resulting acquired skills.

To examine the subjects' initial skills level, we analysed the smoothness and accuracy using a 2-way ANOVA with two in-between predictors – partner and stiffness. We conducted tailored post-hoc comparisons using t-test contrasts to investigate the differences between the single factor levels. Moreover, a Dunnett test was conducted to compare each condition to a control group. The Benjamini–Hochberg adjustment was used to control the false discovery

rate resulting from multiple comparisons. Since all 13 groups were not different in the performance (all $p>0.06$), in following analysis this skills baseline was not considered.

To investigate performance during the training we conducted a 3-way mixed ANOVA with two in-between factors – partner and stiffness condition, and with one repeated measures predictor – training trial. We used tailored t-test contrasts with Benjamini–Hochberg adjustment to investigate the difference between the groups in the last five trials and within the same groups between different training trials. The differences between different trials in the solo group were analysed with paired t-tests. The comparisons between the S and other groups were realised using Dunnett tests.

To investigate how training with shared control influenced the learning, we analysed the smoothness and accuracy in the retention and transfer trials immediately, one day and one week after training. Due to the presence of missing observations in the data for some of the post-tests and non-normal data distribution in some of the conditions, we conducted an ANOVA using a linear mixed-effects model. For all dependent variables, we fitted a model with fixed effects on the stiffness, partner condition, test time (immediately after training, one day or one week after) and their interactions, and the random intercepts for the subject number. When one of the factors or their interaction was significant, post-hoc comparisons using t-test contrasts with a Benjamini–Hochberg adjustment were employed. A Dunnett test was conducted to compare each condition to the control group.

Chapter 2

Adapting impedance to improve haptic communication

Carrying a table together, shared driving, and physical rehabilitation, all involve a human and a robot agent physically interacting to achieve a common goal. Can interacting agents harness their mechanics to improve their perception of the partner and thus their performance? Successful techniques have been developed to shape the energy transfer between agents but it is unclear how to improve the sensory information exchange. In this chapter, we analyze the interaction dynamics of two agents considering the stochastic properties of their sensory signals, and how their combination depends on mechanical impedance. Using stochastic nonlinear optimal control theory, we develop a strategy for shaping the information exchange in interacting soft agents and optimizing their sensory prediction. To systematically test this stochastic optimal information and effort (SOIE) control, we first implemented on a pair of connected robots, where performance was compared with a constant impedance controller. The results indicate that the SOIE control achieves better tracking accuracy with comparable effort, by perceiving the target information from the partner interaction. Second, we showed that the SOIE model could predict the adaptation observed in interacting humans. Finally, the use of SOIE control was experimentally tested for human-robot interaction on twelve subjects. The data shows that the tracking error and effort on both the human and robot sides were improved compared to maximal impedance control when the robot is subjected to noise. These results demonstrate that the adaptive controller introduced in this chapter can improve the perception of target movement by optimally integrating own and the partner's sensory information.

Could interacting agents harness their mechanics to improve their perception? Successful techniques have been developed to shape the energy transfer between agents [35, 36, 37], but it is unclear how to improve sensory information exchange. In this chapter, we first analyse the interaction dynamics of two agents considering the stochastic properties of their sensory signals, and how their combination depends on the mechanical impedance (i.e. the transfer function from position state to force [38]). Using stochastic nonlinear optimal control theory, we develop a strategy for shaping the information exchange in interacting soft agents and optimizing their sensory prediction. We then systematically test the resulting controller on a pair of connected robots, and to implement efficient human-robot interaction.

Stochastic nonlinear optimal control of physical interaction

We consider two agents that can apply forces on the environment or on each other and tune their control impedance, such as a robot and its human user. We assume that these *soft agents* are equipped with (i) exteroception (e.g. in the form of vision, lidar or ultrasound) to locate objects of interest relative to their own position, and (ii) sensing of the interaction force with a partner or the environment. As a prototype task requiring continuous control, we consider the tracking of a common target by two agents connected through an elastic band (Fig.2.1A). Without loss of generality, we consider in the following a robot in contact with its human operator. We will derive the robot control law, while the human control can be modelled similarly.

The task's goal is to track a target moving according to $\eta(t) \in \mathbb{R}^n$ with time t. We suppose that, using exteroception with noise $\nu \in \mathcal{N}(\delta_\nu, \Sigma_\nu)$, the robot predicts the target motion $\hat{\eta}$ and generates control commands to track it according to:

$$u(t) \equiv \psi\left[\hat{\eta}(t), \hat{\dot{\eta}}(t), \hat{\ddot{\eta}}(t)\right] + \phi(t) + \zeta\,. \tag{2.1}$$

The *motor command* u consists of a *feedforward part* $\psi(\hat{\eta}, \hat{\dot{\eta}}, \hat{\ddot{\eta}})$ that has typically been learned to provide the robot's dynamics, a *feedback part* ϕ to reduce online deviations, and Gaussian motor noise $\zeta \in \mathcal{N}(0, \Sigma_\eta)$, where all these variables are vectors of dimension n.

The robot dynamics ψ are driven on the robot joint trajectory $q(t) \in \mathbb{R}^n$ by the motor command u and the interaction torque τ with the human:

$$\psi\left[q(t), \dot{q}(t), \ddot{q}(t)\right] = u(t) + \tau(t)\,. \tag{2.2}$$

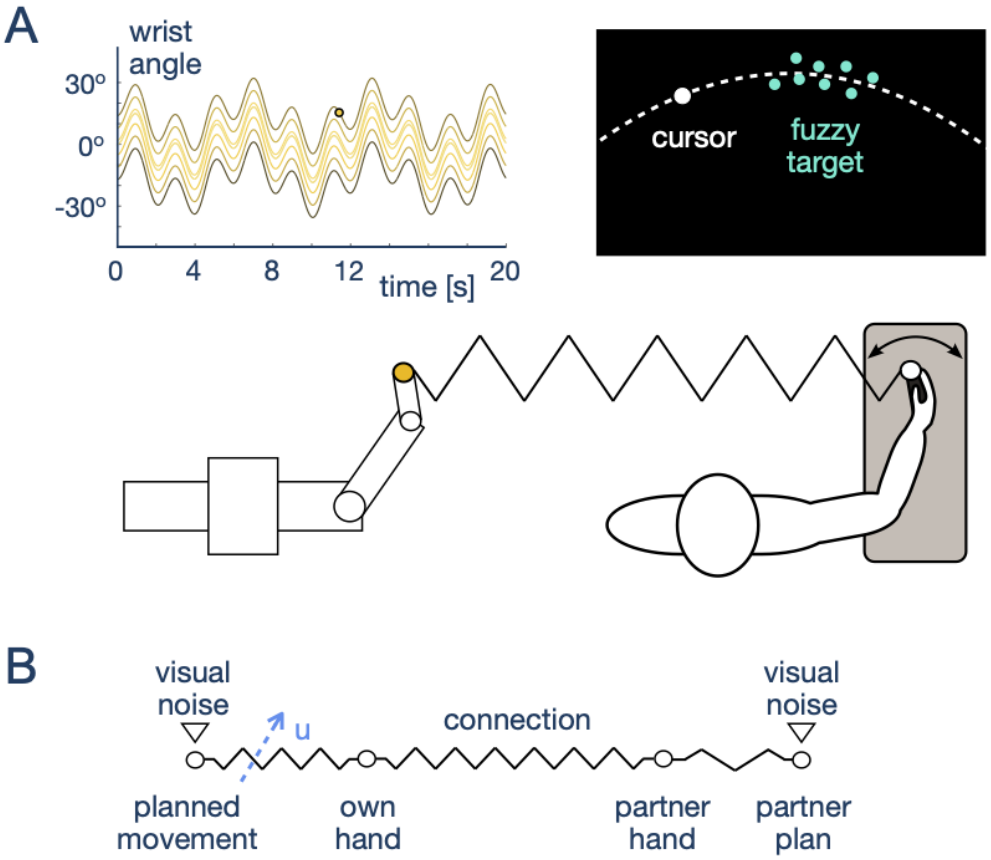

Figure 2.1: **Human and robot agents collaborating on a tracking task while exchanging energy and information through an elastic band. (A) Each agent perceives the target movement relative to their own position and the interaction force with the partner, and is subjected to respective noises and to motor noise. (B) Each of these soft agents can adapt their control impedance for following own planned trajectory to track the target, while considering the partner's movement toward the same target as perceived from the interaction.**

Let these dynamics be linearized around the predicted target $\hat{\eta}(t)$:

$$\begin{aligned} \psi(q,\dot{q},\ddot{q}) \;\cong\; \psi(\hat{\eta},\hat{\dot{\eta}},\hat{\ddot{\eta}}) + K\xi + D\dot{\xi} + I\ddot{\xi}\,, \\ \xi \equiv q-\hat{\eta}\,, \quad \dot{\xi} \equiv \dot{q}-\hat{\dot{\eta}}\,, \quad \ddot{\xi} \equiv \ddot{q}-\hat{\ddot{\eta}} \end{aligned} \tag{2.3}$$

where K, D and I are stiffness, viscosity and inertia matrices respectively, and the time variable has been omitted for clarity. K, D, I are changing slowly with the position state, and we assume that they are constant. Using eqs.(2.1-2.3), the robot's interaction with the human can be expressed in state space as

$$\begin{aligned} \dot{z} = Az + B(\phi+\tau) + B\,\zeta\,, \quad z \equiv \begin{bmatrix} \xi \\ \dot{\xi} \end{bmatrix}, \\ A \equiv \begin{bmatrix} 0_n & 1_n \\ -I^{-1}K & -I^{-1}D \end{bmatrix}, \quad B \equiv \begin{bmatrix} 0_n \\ I^{-1} \end{bmatrix}. \end{aligned} \tag{2.4}$$

where 1_n is the $n\times n$ identity matrix and 0_n is formed of 0 components.

The feedback control component

$$\phi = -L'z \tag{2.5}$$

uses (the transpose of) the impedance control vector L to execute the planned movement to track the target by reducing the tracking error z. Finally, we assume that the two agents are related by

$$\tau = -\tilde{\tau} \;=\; H \begin{bmatrix} \tilde{q}-q \\ \dot{\tilde{q}}-\dot{q} \end{bmatrix} = H(\tilde{z}-z+\varepsilon)\,, \quad \varepsilon \equiv \hat{\eta}-\tilde{\hat{\eta}} \tag{2.6}$$

where the subscript $\tilde{}$ is used to denote the partner's variables. The $n\times 2n$ matrix H specifies the connection viscoelasticity, and the degradation of haptic sensibility with the connection compliance [4] is modelled as Gaussian noise $\in \mathcal{N}(0,\Sigma_H)$.

Combining eqs.(2.4-2.6), the closed-loop dynamics of target tracking yields

$$\dot{z} = \bar{A}z - BL'\nu + BH\mu + B\,\zeta\,, \quad \bar{A} \equiv A - BH - BL' \tag{2.7}$$

where ν is exteroceptive noise and $\mu \equiv \tilde{z}+\varepsilon$ is considered as haptic noise, modelled as a Gaussian biased noise $\mu \in \mathcal{N}(\delta_\mu,\Sigma_\mu)$. Both μ and ζ act as perturbations to the robot tracking dynamics.

How should the control impedance L be selected? On the one hand, it should reduce the tracking error. On the other hand, coupled with the sensory noise, it would amplify the perturbation and thus increase both the error and control effort. To consider this trade-off, we assume that L is adapted to minimize the error and effort

$$J = \mathbb{E}\left[z'(T)Q_T z(T) + \int_0^T [z'(t)Qz(t) + L'(t)RL(t)]\, dt \right] \tag{2.8}$$

In this cost function, $\mathbb{E}[\cdot]$ denotes the expected value, the movement is from time $t = 0$ to $t = T$, R is a positive definite matrix and Q, Q_T are positive semi-definite matrices. This is similar to the cost function commonly used to model human motor control [12] with an added consideration of the stochastics of the sensory signals.

As in eq.(2.8) the system states, control variable and noise are coupled, this yields a nonlinear stochastic optimal control problem which can be solved using the method of [39]. We assume that the system has an initial error distribution and Gaussian distributed noises. As the tracking error dynamics eq. (2.7) is a bilinear stochastic differential equation, the state evolution will be a Gaussian process determined by propagation of its mean $m(t) \equiv \mathbb{E}[z(t)]$ and covariance $P(t) \equiv \mathbb{E}\{[z(t) - m(t)][z(t) - m(t)]'\}$:

$$\begin{aligned} \dot{m} &= \bar{A}\, m - BL'\delta_\nu + BH\delta_\mu \\ \dot{P} &= \bar{A}P + P\bar{A}' + BL\Sigma_\nu L'B' + \Omega_\mu + \Omega_\eta \\ \Omega_\mu &\equiv BH\Sigma_\mu H'B', \quad \Omega_\eta \equiv B(\Sigma_\eta + \Sigma_H)B'. \end{aligned} \tag{2.9}$$

The cost function eq. (2.8) is then represented as

$$\begin{aligned} \bar{J} = {} & m(T)'Q\, m(T) + tr(Q_T P_T) + \\ & \int_0^T [\, m'(t)\, Q\, m(t) + L'RL + tr(QP(t))]\, dt\,. \end{aligned} \tag{2.10}$$

The stochastic optimal control problem of eqs.(2.7,2.8) has been converted to the deterministic optimal control problem of eqs.(2.9,2.10) with the mean and covariance of the tracking error as states, which can be solved using Monte Carlo sampling-based methods [40].

The developed *stochastic optimal information and effort model* (SOIE) was implemented on the Hi5 dual robotic interface of [29] illustrated in Fig. 2.1A. Equipped with two wrist flexion/extension handles actuated independently and torque and angle sensors at both sides. This dual interface enabled us to systematically investigate interactions between two human/robot agents. We report in the next two sections experiments with SOIE on robot-robot collaboration and the effect on human-robot interaction.

Impedance adaptation in two robot collaboration

A first experiment was carried out to systematically test the SOIE algorithm on two robots connected by a virtual elastic band of stiffness 17.2 Nm/rad. The task consisted of tracking a target moving with

$$q^*(t) \equiv 18.5\,\sin(2.031\,t^*)\,\sin(1.093\,t^*)\,, \qquad (2.11)$$
$$t^* \equiv t + t_0\,, \quad 0 \le t \le 20\,s\,, \quad t_0 \in \{[0,20]s \,|\, q^*(t_0) \equiv 0\}$$

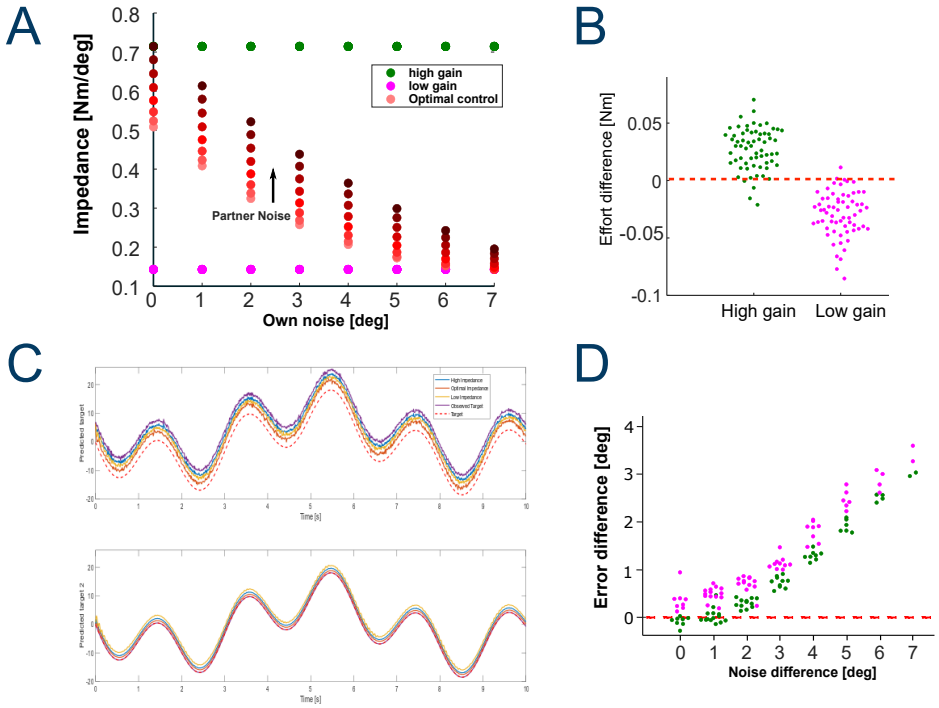

Figure 2.2: **Impedance adaptation in robot-robot interaction. Panel A shows how optimal impedance varies with one's own and with partner noise. Panel B compares the effort between the optimal impedance and the low or high constant impedance. Panel C compares the prediction of target trajectory in interacting robots, the top with with 7° bias and the bottom without bias, where optimal impedance yields superior prediction in both cases. Furthermore, the average tracking error in 10 interaction trials shown in panel D exhibits improved tracking performance.**

using the exteroception and interaction force measured at each robot. Exteroception was implemented in each robot as the target trajectory subjected to biased Gaussian noise with standard deviation $\sigma_\nu = 0.05°$ and mean $\delta_\nu \in \{0°, 1° \dots 7°\}$. One trial was carried out for each of the $8 \times 8 = 64$ conditions. Performance was evaluated using two metrics. The *tracking error*

$$\left(\frac{1}{T}\int_0^T [q^*(t) - q(t)]^2\, dt\right)^{\frac{1}{2}}, \quad T \equiv 10\, s \tag{2.12}$$

was computed over each trial, and the tracking performance was evaluated using the sum of errors in the two robots. Furthermore, *effort* over one trial was evaluated from

$$\left(\frac{1}{T}\int_0^T \tau(t)^2\, dt\right)^{\frac{1}{2}}, \quad T \equiv 10\, s\,. \tag{2.13}$$

We see in Fig. 2.2A that the SOIE algorithm can adapt impedance to each noise condition of the two partners, by decreasing with own noise and increasing with the partner noise level. Controllers with low and high impedance were also tested for comparison. Fig. 2.2B shows that the effort relative to SOIE decreases with minimum impedance ($p<0.001$, paired T-test) and increases with maximum impedance ($p<0.001$, paired T-test) relative to the value selected by SOIE. However, as appears in Fig. 2.2C, in both cases the sensory prediction from eq. (2.5) is worse than with SOIE for both robot agents with biased (top) and unbiased (bottom) proprioception. Furthermore, as shown in Fig. 2.3, the target information exchanged between the partners through interaction torque correlates (Pearson correlation $r = 0.89$) with the target movement when using SOIE but not well with either maximum ($r = 0.14$) or minimal ($r = 0.53$) impedance. Therefore, SOIE yields higher signal-to-noise ratio transmission ($SNR = 6.99\,\text{dB}$) than the maximum ($SNR = -2.76$ dB) and minimum ($SNR = -0.57\,\text{dB}$) impedance. Similarly, the phase shift of the target trajectory in optimal impedance (0.24 s) is lower than maximum and minimal impedance (0.56 s and 0.64 s respectively). These results indicate that SOIE improves the target information exchange relative to fixed impedance control.

Fig. 2.2D shows that the resulting error is larger relatively to SOIE with both fixed low impedance ($p<0.001$, paired t-test) and high impedance ($p<0.001$). The tracking error difference to the optimal control contribution increases linearly with the noise difference to the partner ($r=0.958$ and $r=0.956$ for the error difference with low and high impedance respectively). This demonstrates the usefulness of considering the deviation of own and the partner's sensing to select impedance accordingly.

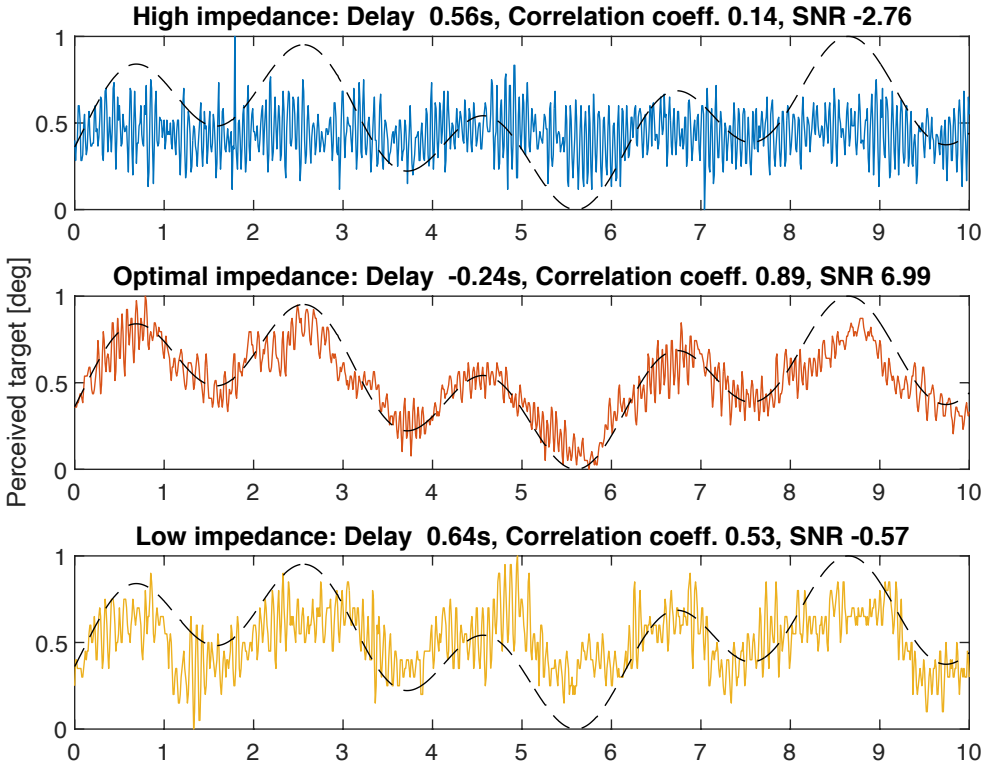

Figure 2.3: **The comparison of perceived target from interaction torque among three controllers: the optimal impedance includes more target movement information than the high impedance and low impedance provides, as can be analysed through the correlation as well as transmission signal to noise ratio and delay.**

Body adaptations in human-human interaction

Would humans adapt their impedance to perceive their partners' movements in an optimal way as predicted by SOIE when they are physically connected in a collaborated tracking task? Chapter 1 of Deliverable 4.1 has reported how subjects connected with a rigid virtual elastic band adapted their wrist flexion/extension co-contraction to improve tracking a common randomly moving target. The experiment was performed with four conditions for a dyad of participants: sharp (self) - noisy (partner) (SN), sharp - sharp (SS), noisy - sharp (NS) and noisy - noisy (NN).

We see in Fig. 2.4A that the cocontraction values from simulations with the SOIE model correspond well to the experimental values for the four noise

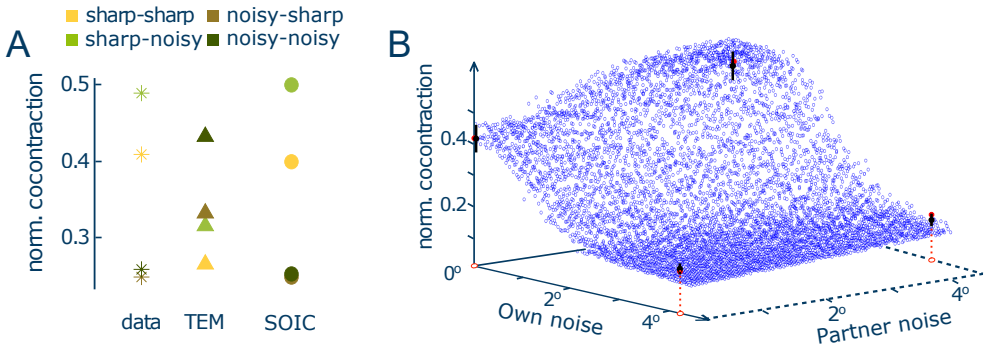

Figure 2.4: **Results of computational modeling the cocontraction adaptation to own and partner noise. (A) Comparison of predicted muscle cocontraction values by TEM and SOIE. The SOIE model predicts well the muscle cocontraction data in four noise conditions where the tracking error minimization (TEM) model fail as it does not consider intrinsic noises. (B) SOIE can predict muscle cocontraction values to different noise combinations, with a decreasing trend to own noise and increase trend to partner noise.**

conditions. In contrast, the *tracking error minimization* (TEM) model, corresponding to the hypothesis that the tracking performance is due to the mechanical effect of the guidance, cannot predict correct trends of tracking error. The SOIE can be used to predict how cocontraction will be modulated on different levels of own visual noise and partner's noise (blue surface of Fig.2.4.B). These results show that interacting humans consider respective noise characteristics to adapt their muscle cocontraction for maximising the information transfer with their partner.

Human-robot impedance adaptation for collaboration

To evaluate the performance of the SOIE algorithm for human-robot interaction on a common task, it was implemented on one of the handles of the Hi5 dual robotic interface [29] connected to the human subject by a virtual elastic band. Both the human and robot had to track a target moving according to (in degree):

$$q^*(t) \equiv 18.5 \sin(3.04\, t^*) \sin(2.51\, t^*), \quad t^* \equiv t + t_0, \quad 0 \leq t \leq 20\, s \quad (2.14)$$

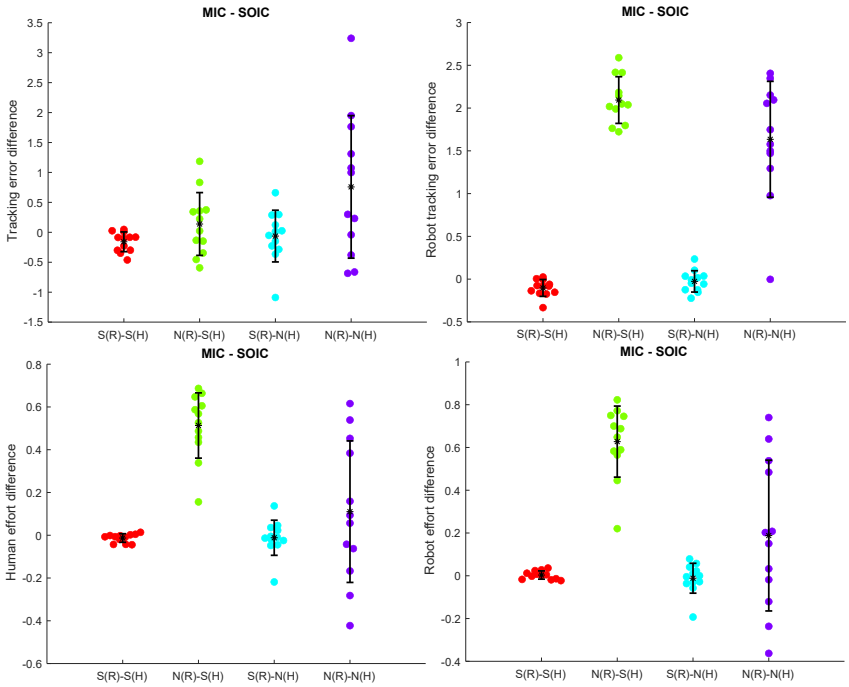

Figure 2.5: **Comparison of tracking error and effort of human and robot in SOIE relative to maximal impedance control (MIC).**

To prevent the participants from memorizing the target's motion, t^* started in each trial from a randomly selected zero $\{t_0 \in [0, 20]s \mid q^*(t_0) \equiv 0\}$ of the multi-sine function.

Trials were carried out in four noise conditions: {SN $\equiv$ robot with sharp target information & human with noisy target, NS, SS, NN}. In the *sharp human condition* the target was displayed as a 8 mm diameter disk, while in the *noisy human condition* the target was a "cloud" of eight normally distributed dots around the target. In the *noisy robot condition* biased Gaussian noise with mean $\delta = 7.01°$ and standard deviation $\sigma = 0.05°$ was added to the reference target trajectory while in the *sharp robot condition* the accurate target trajectory was passed to the robot. Interaction with SOIE was compared with interaction with a maximal impedance controller. The impedance of SOIE is computed from the optimization of the cost eq. (2.10), which is adapted to the own and partner noises as shown in Fig. 2.2A. The maximal impedance control uses the maximal impedance in Fig. 2.2A and was kept constant during all noise conditions. Each subject had an initial 10 solo trials to familiarise themselves with the task and interface dynamics, followed by 4

blocks of 10 interaction trials with one controller, and another 4 blocks of 10 trials with the other controller. The order of two controllers was randomized within the subjects group, and the 4 blocks of each controller corresponds to 4 randomized noise conditions.

Fig. 2.5 presents the tracking error eq.(2.12) and effort eq.(2.13) on the human and robot agents in the last trial. We see in the left panels that the tracking error and effort of the human agent are similar in SOIE as with maximal fixed impedance when the robot has sharp sensing (in the SS and SN conditions). This result stems from the high gains of both controllers so that the subjects can rely on robot guidance, as was verified from the low muscle activation observed in this case. When the robot has noisy sensing (in the NS and NN conditions), SOIE results in smaller average tracking error and effort. The robot side presented in the right panels of Fig. 2.5 exhibits similar tendencies with more marked results and a significant improvement of tracking performance with less effort. This demonstrates the efficiency of impedance adaptation using SOIE.

Discussion

Previous controllers for multi-agent physical interaction considered the energy exchange through the haptic channel [35, 36], but did not examine the associated information transfer. However, recent studies have revealed how interacting humans harness their body properties to share sensory information through this channel considering the respective noise properties, thereby improving their sensory prediction and performance [3][D4.1 Chapter 3]. Deterministic methods for sensor-based control, such as linear quadratic regulation, generate optimal commands that are not appropriate to consider the noise in interacting sensorimotor systems.

Therefore, we have analyzed the intermingled dynamics of mechanical properties and stochastic sensory signals during the physical interaction of soft agents, and the sensor fusion across their connection. As a result, we have derived a stochastic nonlinear optimal information and effort controller (SOIE) considering both the energy and information exchange of physically interacting soft agents such as humans and robots.

The noise dependent adaptation of mechanical impedance observed by humans is not explained by existing models according to which stiffness increases with the magnitude of error to the planned trajectory [12, 41, 42, 43].

The SOIE controller extends these previous motor learning and adaptation models by showing how the CNS adapts body stiffness to minimize the error, effort and their variance. Our simulation results showed that this controller can predict the impedance adaptation in interacting humans by considering the coupling effect between the noise and mechanical impedance as well as the state/control dependent noise.

Maximum likelihood estimation methods have previously been used to predict the trial-by-trial evolution of movement error [44, 45] or mechanical impedance (D4.1, Chapter 3) in humans. However, these methods do not consider the interaction dynamics during movement. Because the SOIE model considers such dynamics between agents and their limb's neuromechanics, it can predict the interaction force, the subsequent muscle activity and tracking error during motion as demonstrated in the above results.

This real-time aspect makes the SOIE an interactive controller for physical human-robot interaction scenarios in which the agent's position is affected by both the agent's own input and the input of their partner. Through the assumption that interacting agents consider own sensory noise, the partner's noise and trajectory uncertainty in addition to the interaction dynamics, the SOIE model determines a control gain that minimizes the expected tracking error and effort as was experimentally demonstrated.

Methods

Monte-Carlo sampling method for impedance optimisation

Human subjects or a robot can modulate the mechanical impedance by changing muscle co-contraction or control gains in eq. (2.5): $L = \Lambda_0 \lambda$, $\Lambda_0 = [\alpha, \beta]$ where $\alpha,\ \beta > 0$ are tuning parameters and λ is the impedance parameter. Due to the existence of own noise $\tilde{\nu}$ in the experiment, the partner's noise $\tilde{z}$ can be approximated as a Gaussian non-zero mean stochastic variable $\tilde{z} \in \mathcal{N}(\delta_h, \Sigma_h)$.

To obtain the optimal impedance λ^*, eq. (2.10) is used to convert the cost function into deterministic values with the evolution of mean and covariance eq. (2.9). Because visual noise ν, haptic noise $\tilde{z}$ and trajectory noise ζ are stochastic variables, a Monte Carlo simulation with 500 trials is conducted to estimate mean and covariance: $\hat{m}(t) = z_i(t)/500$, $\hat{P}(t) = e_i(t)e_i(t)'/500$

where $e_i(t) = z_i(t) - \hat{m}(t)$ and $i = 1, 2, ..., 500$. The optimal mechanical impedance is then determined from

$$\lambda^* = {}_{\lambda\in[0,0.6]}\bar{J}(\hat{m}, \hat{P}), \tag{2.15}$$

where the equivalent deterministic cost is

$$\bar{J}(\hat{m}, \hat{P}) = \sum_{i=1}^{N} \left[\hat{m}_i' \, Q \, \hat{m}_i + \lambda_i' \, R \, \lambda_i + tr(Q\hat{P}_i) \right].$$

Robot-robot experiment protocol

Each handle of the Hi5 dual robotic interface used in the experiments [29] is connected to a current-controlled DC motor (MSS8, Mavilor) that can exert torques of up to 15 Nm, and is equipped with a differential encoder (RI 58-O, Hengstler) to measure the wrist angle and a (TRT-100, Transducer Technologies) sensor to measure the exerted torque in the range [0,11.29] Nm. The two handles are controlled at 1 kHz using Labview Real-Time v14.0 (National Instruments) and a data acquisition board (DAQ-PCI-6221, National Instruments), while the data was recorded at 100 Hz.

Each robot had two noise conditions: in the *sharp condition* the target reference trajectory was directly tracked by the robot, while in the noisy condition a 7.01° biased target position was passed to the controller. Each robot handle was programmed by using the developed SOIE adaptive controller that optimizes the cost eq. (2.10) considering the dynamics eq. (2.9). For comparison, two controllers with fixed high/low impedance were used. The experiment consisted of 12 blocks of 10 interactive trials. The three controllers were used in random order with 4 blocks corresponding to the noise conditions {SS, SN, NS, NN}.

The signal-to-noise ratio is defined as the ratio of the power of a signal to the power of noise:

$$SNR = 10 \log_{10} \left(\frac{P_{\text{signal}}}{P_{\text{noise}}} \right) \tag{2.16}$$

where P_{signal} and P_{noise} are the average signal and noise power, respectively.

Simulation of human-human interaction

The experiment of collaborative tracking of a randomly moving target described in Chapter 1 of Deliverable 4.1 was simulated with SOIE using the

parameters of Table 1.

Table 1: Parameters used in simulations

Symbols	**Physical meaning**	**Values**	**Units**
t_f	task duration	20	s
dt	step	0.01	s
ξ_0	initial error	[0.01, 0]	[rad,rad/s]
I	wrist inertial	0.34	kg$\cdot$ rad^2
b	wrist viscosity	0.02	kg$\cdot$ rad$^2/s$
k	wrist stiffness	0.1	kg$\cdot$ rad^2/s^2
Σ_ν	visual noise cov.	$\begin{bmatrix} 0.018 & 0 \\ 0 & 0.00018 \end{bmatrix}$	rad^2
Σ_η	trajectory noise cov.	$\begin{bmatrix} 0.035 & 0 \\ 0 & 0.00035 \end{bmatrix}$	rad^2
$[\alpha, \beta]$	human control vector	[2, 0.2]	Nm/rad
Q	error weight matrix	$\begin{bmatrix} 1 & 0 \\ 0 & 0.1 \end{bmatrix}$	-
R	effort weight	0.15	-

Human-robot experiment protocol

Human-robot collaboration experiment was approved by the Joint Research Compliance Office at Imperial College London. 12 participants (3 female and 9 male) without known sensorimotor impairments, aged 18–44 years, were recruited. Each participant gave written informed consent prior to participation. The participants carried out the experiment alone. Participant were seated comfortably on height-adjustable chairs, next to the Hi5 dual robotic interface [29]. They held their respective handle with the right wrist

and received visual feedback of the flexion/extension movement on a personal monitor.

The activation of two antagonist wrist muscles, the flexor carpi radialis (FCR) and extensor carpi radialis longus (ECRL) were recorded during the movement from each participant. Electromyographic (EMG) signals were measured with surface electrodes using the medically certified g.Tec's g.LADYBird&g.GAMMABox&g.BSamp system. The EMG data was recorded at 100 Hz.

The experiment consisted of three stages: calibration, solo trials and interactive trials. A calibration of the measured EMG was first carried out to map the raw EMG signal (in mV) to a corresponding torque value (in Nm), so that the activity of each participant's flexor and extensor's can be compared and combined in the data analysis. After this calibration, the participants carried out 10 initial solo trials to learn the tracking task and the dynamics of the wrist interface. This was followed by 8 blocks of 10 interactive trials, where the robot was controlled by the developed SOIE control and a maximal impedance controller randomly in the first 4 blocks and last 4 blocks. For a controller, each with one of the different noise conditions {Noisy(self)-sharp(partner): NS, SN, SS, NN} presented in a random order. The participants were informed when an experimental condition would be changed but not which condition would be encountered in the next trials. The tracking error defined in eq. (2.12) was displayed at the end of each 20 s trial in all trials.

After each trial, the target disappeared and the participants needed to place their respective cursor on the starting position at the center of the screen. The next trial then started after a 5 s rest period and a 3 s countdown. The initialization of next trial started when the participant placed the wrist on the starting position, so that each participant could take a break at will in between trials, by keeping the cursor away from the center of the screen.

In *interactive trials*, the partner's wrist was connected by a virtual spring with stiffness 17.2 Nm/rad to a robotic partner that tracks the same target movement. The interactive torque (in Nm)

$$\tau(t) = 17.2\,[q_p(t) - q_o(t)]\,, \tag{2.17}$$

where q_o and q_p (in radian) denote own and the partner's wrist angles.

The interaction trials were carried out under two different visual feedback conditions on human side. In the *sharp human condition* the target was displayed as a 8 mm diameter disk. In the *noisy human condition* the tar-

get trajectory was displayed as a "cloud" of eight normally distributed dots around the target. The cloud of dots were defined by three parameters, randomly picked from independent Gaussian distributions: the vertical distance to the target position $\eta \in N(0,\, 15\, mm)$, the angular distance to the target position $\eta_q \in N(0,\, 7.01^\circ)$, and the angular velocity $\eta_{\dot{q}} \in \mathrm{N}(0, 10.01^\circ/\mathrm{s})$. Each of the eight dots was sequentially replaced every 100 ms. Two haptic noise conditions were presented from robot side. In *noisy robot condition* there is biased Gaussian noise with mean $\delta = 7.01^\circ$ and standard deviation $\sigma = 0.05^\circ$ added to the reference target trajectory while the accurate target trajectory is given to the robot for tracking in *sharp robot condition*.

Chapter 3

Asymmetric connection between humans can improve performance with little effort

Physical interaction between individuals performing a common motor task leads to performance improvement as individuals exchange haptic information [3]. However, the performance improvement and the interaction effort vary with the connection stiffness and the relative skill level of the partners [4]. Here we i) extend previous results on human-human physical interaction by studying the effect of high (H) and low (L) asymmetric connection stiffness, resulting in the four conditions {HH, LL, HL, LH}, on the performance of the better and worse partners; ii) consider a 3 DoF tracking task involving translations against gravity and rotation.

The experimental data shows how the asymmetric condition LH (low stiffness for the better partner and high for the worse one) guarantees the highest dyad performance while reducing their effort. It can be argued that decreasing the stiffness for the better partner reduces the negative influence of the partner's movement (and thus decreasing their effort) while still providing sensory feedback for multisensory integration; on the other side, increasing the stiffness on the worse partner positively influences both multisensory integration and guidance from the partner.

These results suggest how to increase the efficiency and efficacy of haptic interaction in scenarios where the motor competencies of the two partners are strongly different, such as a teacher-student interaction in education or a patient-therapist interaction in rehabilitation.

Introduction

Humans rely on physical interaction to learn from each other, by exchanging haptic information during common motor tasks. It has been shown in previous works [1, 2] that in performing joint tasks physical interaction improves performance of the less skilled partner without hindering the motor capabilities of the most skilled one. Importantly, this improvement is modulated by the connection stiffness [4]. A rigid connection yields large performance improvement for the worse partner. While this does not strongly affect the performance of the better partner, it does significantly increase their metabolic cost. To explain these results, it has been proposed that haptic connection acts for both partners as a source for multisensory integration in estimating tracking error, so leading to augmented sensory information and thus fostering better performance [3]. Furthermore, it has been shown in [4] that the higher the stiffness the more reliable is this sensory augmentation. However, the partners' movements are also affected by their interaction force. Arguably, while the augmented sensory feedback and interaction force positively affect the performance of the worse partner, the better partner is helped by multisensory integration but negatively affected by the partner's movements. The better partner can attenuate the disturbance arising from the interaction with a worse partner but at the cost of a higher co-contraction and thus energy.

To understand how to maximise the performance/effort trade-off in connected partners, we investigate in this Chapter if and how asymmetric connection influences the performance of physically interacting individuals with different motor skills. For this purpose the performance of one of the two partners was tuned by adding visual noise on their target, and tested four coupling conditions, using low and high symmetric connections or high/low and low/high asymmetric connections. Our idea is to combine a high stiffness condition for the less skilled subject (sensory augmentation and good haptic guidance) with low stiffness condition for the more skilled subject (marginally deviated by the worse partner) in an attempt to achieve the highest improvement for both subjects with minimal effort. Furthermore, while most previous studies on haptic communication have been carried out on simple 1 dof or 2 dof planar tasks, we extend the paradigm of [1] to 3 DoF movements (2 translations plus 1 rotation) with gravity.

Materials and Methods

Subjects

The study was approved by the Ethics Committee of Università Campus Bio-Medico di Roma (HUROB protocol) and carried out in accordance with the Declaration of Helsinki. 20 healthy volunteers (18 right-handed, aged 22.5 $\pm$ 2.6 years old, 9 female) participated in the study after providing written informed consent. Participants were randomly organized in ten *dyads*, pairing individuals with the same handedness -assessed through an Oldfield test - [33] before starting the experiments.

Setup

Each partner sat in front of a monitor displaying a randomly moving target and a cursor corresponding to their hand movement while being connected to a robotic interface (see Figure 3.1). A curtain separated paired individuals hiding the partner and their setup. Participants were not aware of the task performed by the partner, nor of a possible physical connection with them.

The robot (Panda by Franka Emika) constrained the motion on the DoFs required in the task, i.e. translations in the vertical plane and rotation around the sagittal axis. To this aim, the robot was impedance controlled with low impedance (i.e., "transparent" behavior) along the task directions and high impedance along the constrained directions. A common reference system, centered in the monitor center, was used for both robot movements and task. Cursor translations corresponded to twice end-effector translations, to let participant spacing the entire virtual workspace with feasible arm movements.

Experiment

The participants were required to track a target constrained to the 3 DoFs (2 position and 1 orientation) of the vertical plane with a cursor by moving an ergonomic handle fixed to the robot end-effector (Fig. 3.1A). The task involved translations in the vertical plane xy and rotation ϕ around the sagittal axis z. The target moved with a multi-sine trajectory defined as

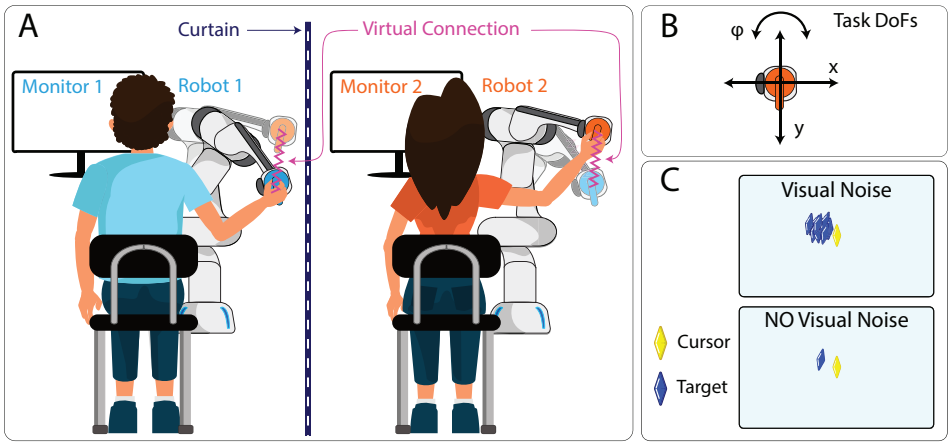

Figure 3.1: **Experiment description. A) Paired participants, separated by a curtain, track the same randomly moving target. Each individual is seated in front of a monitor on which the target and their own cursor are displayed. They control the cursor by guiding the robot end-effector along the task DoFs. The two robots *virtually connect* paired participants' right hand through a visco-elastic force proportional to the difference between their poses. B) Three DoFs involved in the task: translation along the horizontal x axis; translation along the vertical y axis, against gravity; rotation ϕ around the sagittal axis z. C) Task displayed on the monitor with yellow and blue diamonds representing respectively the cursor and the target to be followed. Both the single target (free visual noise condition) and the Gaussian distribution of ten target replicas (visual noise condition) are depicted.**

follows:

$$\begin{cases} x(t) = 6.4\sin(1.8\,t) + 2.5\sin(1.82\,t) + 4.3\sin(2.34\,t) \\ y(t) = 3\sin(1.1\,t) + 3.2\sin(3.6\,t) + 3.8\sin(2.5\,t) + 4.8\sin(1.48\,t) \\ \phi(t) = 20\sin(1.4\,t) + 12\sin(2.5\,t) + 17.5\sin(1.8\,t) + 8.1\sin(2\,t) \end{cases} \quad (3.1)$$

The trajectory had a duration of 30 seconds; for each trial t started from a randomly selected zero $\{t_0 \in [0, 10]s \quad | \quad x(t_0) \equiv y(t_0) \equiv \phi(t_0) \equiv 0\}$ of the multi-sine trajectory. Overall, the target was within a $26{\times}26\,\mathrm{cm}^2$ square workspace with a maximum rotation of ± 55 degrees with respect to the vertical axis.

In order to test partners with a range of different skill levels, the individuals' skill to carry out the task was modulated through the addition of Gaussian visual noise on the target of one partner per dyad [5]. In particular, target was

replaced by a cloud of ten replicas normally distributed around the desired pose -x, y and ϕ- with a standard deviation equal to 2 cm for position (x and y) and 8° for orientation (ϕ). These values were chosen through a preliminary *Visual Noise Experiment* described in more detail in *Visual Noise Estimation* section. To balance the experimental condition, the same 20 participants underwent a second experimental session with the other partner having visual noise. Thus, the overall pool considered in the data analysis was composed of 20 different dyads.

Partners were virtually connected through a visco-elastic force/torque $\mathbf{F}$ proportional to the difference between their pose $\mathbf{p}$:

$$\begin{aligned}\mathbf{F}_i = \begin{bmatrix} F_{x,i} \\ F_{y,i} \\ \tau_{\phi,i} \end{bmatrix} &= \mathbf{K}_i(\mathbf{p}_j - \mathbf{p}_i) + \mathbf{D}_i(\dot{\mathbf{p}}_i) = \\ &= \begin{bmatrix} K_{x,i} & 0 & 0 \\ 0 & K_{y,i} & 0 \\ 0 & 0 & K_{\phi,i} \end{bmatrix} \left(\begin{bmatrix} x_j \\ y_j \\ \phi_j \end{bmatrix} - \begin{bmatrix} x_i \\ y_i \\ \phi_i \end{bmatrix} \right) + \\ &+ \gamma \begin{bmatrix} \sqrt{K_{x,i}} & 0 & 0 \\ 0 & \sqrt{K_{y,i}} & 0 \\ 0 & 0 & \sqrt{K_{\phi,i}} \end{bmatrix} \begin{bmatrix} \dot{x}_i \\ \dot{y}_i \\ \dot{\phi}_i \end{bmatrix};\end{aligned} \tag{3.2}$$

where $\dot{\mathbf{p}}$ is the velocity vector and the subscripts $i, j \in \{1, 2\}$, $i \neq j$, indicate the dyad member the vectors are referred to. The haptic force was composed by two linear force F_x and F_y acting along x and y, and a torque τ_ϕ acting around the rotational axis z. The stiffness matrix $\mathbf{K}$ was set high (H) or low (L): the high stiffness was characterized by $K_x = K_y = 180\,\mathrm{N/m}$ and $K_\phi = 9\,\mathrm{Nm/rad}$; the low one had $K_x = K_y = 60\,\mathrm{N/m}$ and $K_\phi = 3\,\mathrm{Nm/rad}$. The damping matrix $\mathbf{D}$ was set proportional to square root of $\mathbf{K}$ through the constant $\gamma = 0.005$.

Participants were not advised about the cooperative nature of the task and about the cause of the force, even if they were informed about the possibility to perceive some force on the handle.

Six surface electromyography (EMG) sensors (Trigno$^{\mathrm{TM}}$ Wireless System, Delsys) were employed to measure the activity of six arm muscles -three flexors and three extensors- involved in the task: Pectoralis major, Posterior

deltoid, Biceps brachii, Lateral Head of Triceps Brachii, Flexor carpi radialis, Extensor carpi radialis longus.

Protocol

Symmetric and asymmetric conditions were tested for the virtual connection, combining low (L) and high (H) stiffness values, respectively assigned to the less skilled partner (performing the task with visual noise) or to the most skilled one, resulting in the four conditions {HH, LL, HL, LH}. During each experimental session dyads underwent the following three phases:

1) *Familiarization*: six *solo* -no physical connection between partners- trials of which three with visual noise and three without, in random order for both partners; 2) *Baseline*: 20 *solo* trials, with visual noise for one partner only; 3) *Test*: 80 trials alternating *solo* and *connected* conditions, all with visual noise for one partner only (the same of the baseline); four stiffness conditions were randomized among the connected trials, resulting in ten repetitions per condition. During the second session visual noise in the *baseline* and *test* conditions was assigned to the other partner.

In all blocks, each trial lasted 30 seconds and was followed by a pause of 10 seconds to avoid the fatigue.

Model

Human-human physical interaction was modeled as in [5]. For each spatial or rotation direction, the dynamic of each subject is described in state-space as:

$$\begin{cases} \mathbf{x}(t+1) = \mathbf{A}\,\mathbf{x}(t) + \mathbf{B}[u(t) + F(t)] \\ \mathbf{z}(t+1) = \mathbf{H}\,\mathbf{x}(t+1) \end{cases} \tag{3.3}$$

where $\mathbf{A} = [1, dt\,;\, 0, 1]$ and $\mathbf{B} = [0\,;\, dt/I]$, with I representing the inertia of the system. $\mathbf{x} = [q, \dot{q}]$ represents the system state vector, with q indicating the difference between target and cursor position/orientation; $\mathbf{z}$ is the state measure obtained from the system state using the selection matrix $\mathbf{H} = [1, 0\,;\, 1, 0]$ and F is the force/torque resulting from the connection between subjects. Considering the subject i, the haptic force is computed using the same formula implemented into the robot control during the experimental sessions: $F_i = [K_i, D_i](\mathbf{x}_j - \mathbf{x}_i)$, $(i, j \in 1, 2$ and $i \neq j)$ using the stiffness and damping values - K_i and D_i - equal to the experimental ones.

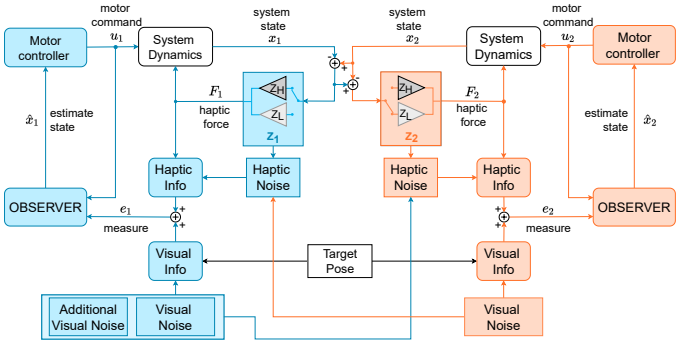

Figure 3.2: **Scheme of *neuromechanical goal sharing* model for two physically connected individuals tracking a common target. Partner represented in blue has additional visual noise to simulate worse motor skills. Connection stiffness (Z) is asymmetric, higher for one partner and lower for the other.**

In the proposed scheme (Fig. 3.2), each subject is represented by the combination of a *Motor Controller* and an *Observer*. The former defines the motor command $u = \mathbf{L}\,\hat{\mathbf{x}} = -[L_p, L_v]\,[\hat{x}; \hat{\dot{x}}]$ needed to move the target interacting with the system, where $\mathbf{L}$ is the vector of control gains for position (L_p) and velocity (L_v), and $\hat{\mathbf{x}}$ is the estimation of the system state obtained from the *Observer*. The *Observer* is composed by an Internal Model of the external system and a Kalman Filter. The Internal Model is described using the dynamic model of the real system (eq. 3.3), supposing the matrices of the internal model ($\tilde{A}, \tilde{B}$) equal to real one, such that $\tilde{A} = A, \tilde{B} = B$. The measure estimation into the Kalman Filter is obtained applying the matrix selection $\mathbf{H}$ on the state estimation $\hat{\mathbf{x}}$. Such estimate is corrected with the measure of the system state $\mathbf{e}$ - difference between target and error position - which is based on both *Visual* and *Haptic Information*. The former is obtained from the screen, whereas the latter is due to the haptic connection force and therefore related to the visual information of the partner. Both the feedback are affected by noise: a base *visual noise* was added to describe the human sensory estimation error, then in the subject with noised visual feedback an *Additional Visual Noise* was added inserting a normal Gaussian disturbance with the same standard deviation used to noise the subject feedback. The noise of the *Haptic Information* is related to both the connection stiffness - the higher the connection, the lesser the noise- and the visual noise of the partner - the higher the visual noise, the higher the haptic noise.

Data Analysis

The position error e was computed as the difference between the target and the cursor separately along x and y; whereas the orientation error was considered as the difference between the target and cursor rotation around the sagittal axis. The root mean square of each error metric was computed along each trial and then used to compute the *Performance Improvement* (I) and the *Partner's Relative Error* (E) indexes, separately for position and orientation [4]. The *performance improvement* is defined as $I = 1 - e_c/e$, where e_c and e indicate the subject's error in two consecutive *connected* and *solo* trials, respectively. Thus, it gives information about the change of the subject's performance, in term of tracking error, between the *connected* and *solo* trials. Considering e_p the partner's error in a *solo* trial and being e computed in the same trial, the *partner's relative error* $E = 1 - e_p/e$ is a metric to evaluate how much the partner is skilled with respect to the subject. Both I and E were computed separately for each DoF and then averaged.

Raw EMG signals were pre-processed through a second order Butterworth band-pass filter in the frequency range $20 - 450\,\text{Hz}$ and a notch filter at $50\,\text{Hz}$, then rectified and finally low pass filtered using a second order Butterworth filter with cut-off frequency of $5\,\text{Hz}$. As for the error, the root mean square value of the filtered EMG data for each sensor was computed for each trial. The obtained filtered EMG data of each sensor i during *connected* trial was normalized with respect to the value obtained from the previous *solo* trial. Then, the root mean square among normalized data of all the sensors was computed obtaining an overall *Interaction Effort* $A = \alpha_c/\alpha - 1$, which gave information about the amount of the effort during *connected* trials with respect to during *solo* trials. Since the first trial of the *Task* block is *connected*, the EMG value of such block were normalized with the last trial in the *Baseline -solo* trial.

Linear mixed models were used to fit with a second order polynomial of both the effort and the improvement with respect to the partner's relative error, for each stiffness condition from {HH, LL, HL, LH}. In particular, the relationship between *improvement* I and *partner's relative error* E was investigated employing a linear mixed-effect model with I as the dependent variable and, E and E^2 as predictors, considering for both E and I the averaged value between position and orientation:

$$I = \beta_0 + \beta_1 E + \beta_2 E^2 + \varepsilon_I \tag{3.4}$$

where β_0 represents the intercept; β_1 and β_2 are the coefficients associated respectively to E and E^2; ε_I is the unexplained variance term associated

to each analysed dyad, considering the same 'physical couple' with different noise condition as two different dyads. A similar analysis was executed to fit the *Effort A* data with respect to the *partner's relative error E*, considering this metric as predictor:

$$A = \delta_0 + \delta_1 E + \varepsilon_A \ . \tag{3.5}$$

The coefficients have the same meaning of the ones in 3.4. Both of these fitting were executed for each stiffness combination {HH, LL, LH, HL}, considering the root mean square data of each trials for all the couples, resulting in four-hundred data for each fitting.

Visual Noise Estimation

The standard deviation of the visual noise used in the experiment was determined from a *Visual Noise Experiment* carried out by six healthy volunteers (all right-handed, aged 30.7 ± 6.9, 3 female) after having signed a written informed consent. They were asked to execute 50 trials of the 3-DoF tracking task in *solo* condition and with visual noise. Four noise levels plus one no-noise condition were randomly presented to the subjects using specific value of standard deviation for position (same value for x and y) and orientation, starting form zero, i.e. no-noise condition. The values of standard deviation (SD) associated to i^{th} noise level for position p and orientation ϕ were computed as: $SD|_{p,i} = i$ cm and $SD|_{\phi,i} = 4i$ deg, where $i \in \{1, 2, 3, 4\}$. We chose the second visual noise level ($i = 2$) since it provided an error almost near to the 10% of the range of motion in both position and orientation.

Haptic Noise Estimation

In [4] it was found that the connection stiffness has an effect on tracking performance similar to noise, with standard deviation increasing with the connection compliance. We conducted a *haptic control experiment* as in [4] to identify the corresponding model parameters taking into account the influence of the connection stiffness on the received information. Eight healthy volunteers (all right-handed, 31.2 ± 2.6 years old, 3 females) participated in the study, after providing written informed consent. They were required to execute the same tracking task of the main experiment (3 DoFs) viewing only their own cursor and not the target. The estimate of the desired pose should be executed by the subjects through the provided haptic force generated by a virtual spring connecting their hand with the target. The stiffness value

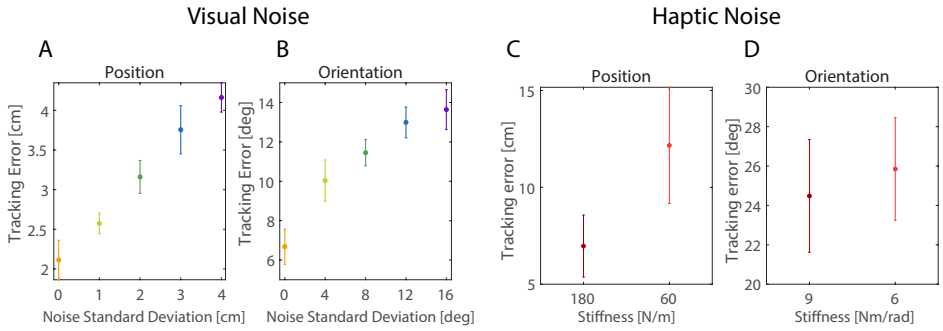

Figure 3.3: **Tracking Error evaluated in term of position (A) and orientation (B) for different amount of the standard deviation related to the visual noise on the target, with zero representing the free noise condition with single target. On the right the tracking error in term of position (C) and orientation (D) evaluated according to the stiffness of the cursor-target connection during a 3-DoFs tracking task with only haptic feedback (and no visual feedback on the monitor).**

of the rotational and linear spring was set high (H) for the first ten trials and low (L) for the last ten trials, considering the stiffness values used in the main experiment. We defined how the two stiffness values influence the target pose estimation analyzing the error in the low and high condition.

Results

Two additional experiments were conducted to estimate model parameters relating tracking errors to the amount of visual noise and connection stiffness, respectively.

The results are shown in Figure 3.3, which depicts the average tracking error, in terms of position and orientation, resulted from the variation of the visual noise standard deviation and connection stiffness respectively.

We see in Fig. 3.4A that the less skilled partner improves in the HH and LH more than in the other conditions ($p < 0.001$), and the converse for the more skilled partners who decrease ($p < 0.001$) more in the HH and HL as in the LL or LH conditions. Additionally, LH is the only condition with no performance deterioration ($I > 0$) for the more skilled individual.

Better partners showed also a large interaction effort in the HH and HL

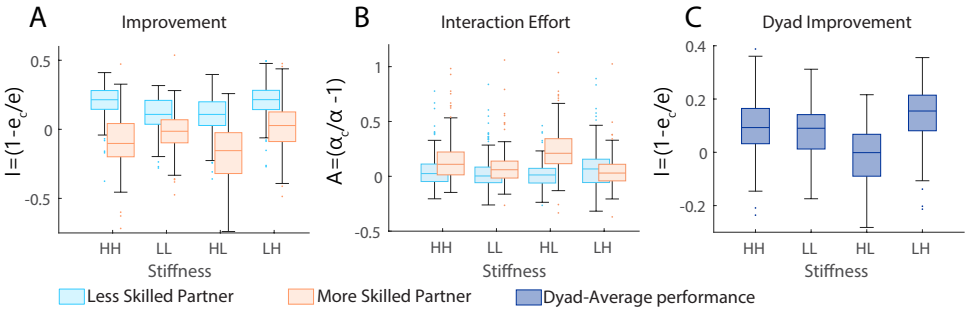

Figure 3.4: **Improvement (A) and interaction effort (B) in the four stiffness conditions (HH,LL,HL,LH), represented in light blue for people performing with visual noise (less skilled partner) and in orange for their partners with no visual noise (more skilled participant). C shows the average improvement within each dyad for the four stiffness conditions. The first stiffness index always refers to the more skilled partner.**

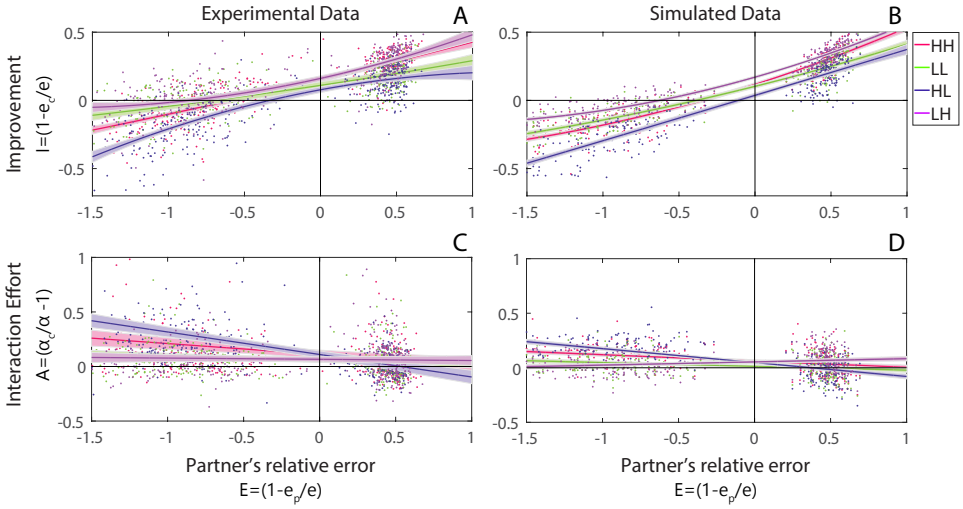

Figure 3.5: **Improvement (A-B) and Interaction Effort (C-D) in the 3 DoF tracking task (average value among x, y and ϕ) with respect to partner's relative error. Data related to one trial and one subject is represented through dots and different colors are used to highlight the four stiffness conditions. Fits for each condition are depicted with solid lines (shadows represent confidence intervals). A and C show experimental data; B and D show data simulated with human-human interaction model from [4].**

conditions compared to the others (Fig. 3.4B). Moreover their effort was significantly larger than the less skilled partners' effort in all cases except for the LH condition where the partners' effort was not significantly different.

We further see in Fig. 3.4C that the average improvement within dyads is significantly larger ($p < 0.001$) in the LH than in all other conditions, whereas there is no significant difference between the HH and LL conditions.

Moreover, post-hoc analysis among the stiffness conditions, regardless the partners' skill, underlines a significant difference in all conditions, with improvement in LH $>$ HH ($p < 0.001$) $>$ LL ($p = 0.041$) $>$ HL ($p < 0.001$).

Looking at the fitting of the experimental data through linear mixed models (Fig. 3.5A,C), indexes of goodness (R^2) were greater than 0.6 in all stiffness cases

Individuals' performance was also simulated using the *neuromechanical goal sharing* model of [4]. This model depicted in Figure 3.2 was previously validated on 2-DoF tracking task with the same connection stiffness (symmetric condition) for partners within the same dyad. Here it was extended to 3-DoFs and asymmetric conditions of the physical interaction. For any stiffness condition dyads' behavior was simulated independently in each dimension and then averaged in the E and I metrics. The obtained values were fitted using the relation eq.(3.4) and obtaining the curves shown in Fig. 3.5.

Indexes of goodness were greater than 0.87 in all stiffness conditions, in terms of improvement; whereas the effort again showed poor fitting goodness, with $R^2 = 0.48$ for HL and $R^2 < 0.17$ otherwise.

Discussion

The new 3 DoF experiment first confirms the the results on human-human physical interaction of previous studies [1, 3, 4, 5], showing that individuals physically coupled while performing a common motor task improve more than if completing the task alone. This result is also valid for movement against the gravity force field, and both in translation and orientation. The quantitative results are further well predicted by the *Neuromechanical goal sharing* model of [4], which was extended to asymmetric stiffness connections.

Importantly, using asymmetric connection stiffness conditions was shown to open opportunities to optimally modulate the physical interaction between

partners. The experimental results confirmed the hypothesis that combining a rigid connection for less skilled partners with a soft one for more skilled partners allows to achieve the best tracking performance for the dyad, with minimal effort.

Conversely, symmetric connection stiffness leads to higher improvement for the worse partner only, while the best partner's performance slightly deteriorates. Most importantly, in this symmetric case the small performance decrement detectable on the highly skilled partner, is obtained at the cost of a large increase in effort from the better partner. In contrast, the asymmetric LH condition yields the dyad with best tracking performance with effort similar as in the solo sessions.

To sum up, physically connecting individuals with asymmetric stiffness - large for the worse partner and low for the better one- maximizes tracking performance without requiring superfluous effort from the partners, i.e. with similar effort as in solo performance.

Bibliography

[1] Gowrishankar Ganesh, Atsushi Takagi, Rieko Osu, Toshinori Yoshioka, Mitsuo Kawato, and Etienne Burdet. Two is better than one: Physical interactions improve motor performance in humans. *Scientific Reports*, 4(1):1–7, 2014.

[2] Niek Beckers, Edwin HF van Asseldonk, and Herman van der Kooij. Haptic human–human interaction does not improve individual visuomotor adaptation. *Scientific Reports*, 10(1):1–11, 2020.

[3] Atsushi Takagi, Gowrishankar Ganesh, Toshinori Yoshioka, Mitsuo Kawato, and Etienne Burdet. Physically interacting individuals estimate the partner's goal to enhance their movements. *Nature Human Behaviour*, 1(3), 2017.

[4] Atsushi Takagi, Francesco Usai, Gowrishankar Ganesh, Vittorio Sanguineti, and Etienne Burdet. Haptic communication between humans is tuned by the hard or soft mechanics of interaction. *PLoS Computational Biology*, 14(3):1–17, 2018.

[5] Atsushi Takagi, Masaya Hirashima, Daichi Nozaki, and Etienne Burdet. Individuals physically interacting in a group rapidly coordinate their movement by estimating the collective goal. *eLife*, 8:1–19, 2019.

[6] Hermano Igo Krebs, Jerome Joseph Palazzolo, Laura Dipietro, Mark Ferraro, Jennifer Krol, Keren Rannekleiv, Bruce T Volpe, and Neville Hogan. Rehabilitation robotics: Performance-based progressive robot-assisted therapy. *Autonomous Robots*, 15(1):7–20, 2003.

[7] Robert Riener, Heike Vallery, and Alexander Duschau-Wicke. Method to control a robot device and robot device, 2014. US Patent 8,924,010.

[8] Marcia K. O'Malley, Abhishek Gupta, Matthew Gen, and Yanfang Li. Shared control in haptic systems for performance enhancement and

training. *Journal of Dynamic Systems, Measurement, and Control*, 128(1):75–85, 2006.

[9] Ekaterina Ivanova, Gerolamo Carboni, Jonathan Eden, Jörg Krüger, and Etienne Burdet. For motion assistance humans prefer to rely on a robot rather than on an unpredictable human. *IEEE Open Journal of Engineering in Medicine and Biology*, 1:133–139, 2020.

[10] Jeremy L. Emken, Raul Benitez, Athanasios Sideris, James E. Bobrow, and David J. Reinkensmeyer. Motor adaptation as a greedy optimization of error and effort. *Journal of Neurophysiology*, 97(6):3997–4006, 2007.

[11] Laura Crespo and David Reinkensmeyer. Effect of robotic guidance on motor learning of a timing task. In *IEEE RAS EMBS International Conference on Biomedical Robotics and Biomechatronics*, pages 199–204, 2008.

[12] David W. Franklin, Etienne Burdet, Keng Peng Tee, Rieko Osu, Chee-Meng Chew, Theodore E. Milner, and Mitsuo Kawato. CNS learns stable, accurate, and efficient movements using a simple algorithm. *Journal of Neuroscience*, 28(44):11165–11173, 2008.

[13] Jaebong Lee and Seungmoon Choi. Effects of haptic guidance and disturbance on motor learning: Potential advantage of haptic disturbance. In *IEEE Haptics Symposium*, pages 335–342, 2010.

[14] Laura Marchal-Crespo, Mathias Bannwart, Robert Riener, and Heike Vallery. The effect of haptic guidance on learning a hybrid rhythmic-discrete motor task. *IEEE Transactions on Haptics*, 8(2):222–234, 2014.

[15] Amine Chellali, Cerdic Dumas, and Isabelle Milleville-Pennel. WYFIWIF: A haptic communication paradigm for collaborative motor skills learning. In *Web Virtual Reality and Three-Dimensional Worlds*, pages 301–308, 2010.

[16] Norma Wegner and Deaman Zeaman. Team and individual performances on a motor learning task. *The Journal of General Psychology*, 55(1):127–142, 1956.

[17] Edwin Mireles, Jacopo Zenzeri, Valentina Squeri, Pietro Morasso, and Dalia De Santis. Skill learning and skill transfer mediated by cooperative haptic interaction. *IEEE Transactions on Neural Systems and Rehabilitation Engineering*, 25(7):832–843, 2017.

[18] Richard A. Schmidt and Timothy D. Lee. *Motor Control and Learning: a behavioral emphasis. 5th Edition.* Human Kinetics, 2011.

[19] Ekin Basalp, Peter Wolf, and Laura Marchal-Crespo. Haptic training: which types facilitate (re) learning of which motor task and for whom answers by a review. *IEEE Transactions on Haptics*, 2021.

[20] Chee Leong Teo, Etienne Burdet, and HP Lim. A robotic teacher of chinese handwriting. In *IEEE HAPTICS*, pages 335–341, 2002.

[21] Laura Marchal-Crespo, Stephanie McHughen, Steven C. Cramer, and David J. Reinkensmeyer. The effect of haptic guidance, aging, and initial skill level on motor learning of a steering task. *Experimental Brain Research*, 201(2):209–220, 2010.

[22] Laura Marchal-Crespo, Mark van Raai, Georg Rauter, Peter Wolf, and Robert Riener. The effect of haptic guidance and visual feedback on learning a complex tennis task. *Experimental Brain Research*, 231(3):277–291, 2013.

[23] Özhan Özen, Karin A. Bütler, and Laura Marchal-Crespo. Promoting motor variability during robotic assistance enhances motor learning of dynamic tasks. *Frontiers in Neuroscience*, 14, 2020.

[24] Reza Shadmehr and Ferdinando A. Mussa-Ivaldi. Adaptive representation of dynamics during learning of a motor task. *Journal of Neuroscience*, 14(5):3208–3224, 1994.

[25] Etienne Burdet, Rieko Osu, David W. Franklin, Theodore E. Milner, and Mitsuo Kawato. The central nervous system stabilizes unstable dynamics by learning optimal impedance. *Nature*, 414:446–449, 2001.

[26] John W. Krakauer. Motor learning and consolidation: the case of visuomotor rotation. *Progress in Motor Control*, pages 405–421, 2009.

[27] Atsushi Takagi, Niek Beckers, and Etienne Burdet. Motion plan changes predictably in dyadic reaching. *PLoS One*, 11(12):e0167314, 2016.

[28] Bastien Berret, Adrien Conessa, Nicolas Schweighofer, and Etienne Burdet. Stochastic optimal feedforward-feedback control determines timing and variability of arm movements with or without vision. *PLOS Computational Biology*, 17(6):e1009047, 2021.

[29] Alejandro Melendez-Calderon, L. Bagutti, B. Pedrono, and Etienne Burdet. Hi5: A versatile dual-wrist device to study human-human interaction and bimanual control. *2011 IEEE International Conference on Intelligent Robots and Systems*, pages 2578–2583, 2011.

[30] Dane Powell and Marcia K. O'Malley. The task-dependent efficacy of shared-control haptic guidance paradigms. *IEEE Transactions on Haptics*, 5(3):208–219, 2012.

[31] Mark Mulder, David A. Abbink, and Erwin R. Boer. Sharing control with haptics: Seamless driver support from manual to automatic control. *Human Factors*, 54(5):786–798, 2012.

[32] Edmund Field and Don Harris. A comparative survey of the utility of cross-cockpit linkages and autoflight systems' backfeed to the control inceptors of commercial aircraft. *Ergonomics*, 41(10):1462–1477, 1998.

[33] Richard C. Oldfield. The assessment and analysis of handedness: The edinburgh inventory. *Neuropsychologia*, 9(1):97–113, 1971.

[34] Sivakumar Balasubramanian, Alejandro Melendez-Calderon, Agnes Roby-Brami, and Etienne Burdet. On the analysis of movement smoothness. *Journal of Neuroengineering and Rehabilitation*, 12(1):112, 2015.

[35] Gennaro Raiola, Carlos Alberto Cardenas, Tadele Shiferaw Tadele, Theo De Vries, and Stefano Stramigioli. Development of a safety-and energy-aware impedance controller for collaborative robots. *IEEE Robotics and Automation Letters*, 3(2):1237–1244, 2018.

[36] Yanan Li, Gerolamo Carboni, Franck Gonzalez, Domenico Campolo, and Etienne Burdet. Differential game theory for versatile physical human–robot interaction. *Nature Machine Intelligence*, 1(1):36–43, 2019.

[37] Zhijun Li, Junqiang Liu, Zhicong Huang, Yan Peng, Huayan Pu, and Liang Ding. Adaptive impedance control of human–robot cooperation using reinforcement learning. *IEEE Transactions on Industrial Electronics*, 64(10):8013–8022, 2017.

[38] Neville Hogan. Impedance control: An approach to manipulation. *Journal of Dynamic Systems, Measurement, and Control*, 107(1):1–17, 1985.

[39] Bastien Berret and Frederic Jean. Efficient computation of optimal open-loop controls for stochastic systems. *Automatica*, 115:108874, 2020.

[40] Tito Homem-de Mello and Güzin Bayraksan. Monte carlo sampling-based methods for stochastic optimization. *Surveys in Operations Research and Management Science*, 19(1):56–85, 2014.

[41] Keng Peng Tee, David W. Franklin, Mitsuo Kawato, Theodore E. Milner, and Etienne Burdet. Concurrent adaptation of force and impedance in the redundant muscle system. *Biological Cybernetics*, 102(1):31–44, 2010.

[42] Evangelos Theodorou, Jonas Büchli, and Stefan Schaal. A generalized path integral control approach to reinforcement learning. *Journal of Machine Learning Research*, 11:3137–3181, 2010.

[43] Yanan Li, Gowrishankar Ganesh, Nathanaël Jarrassé, Sami Haddadin, Alin Albu-Schaeffer, and Etienne Burdet. Force, impedance, and trajectory learning for contact tooling and haptic identification. *IEEE Transactions on Robotics*, 34(5):1170–1182, 2018.

[44] David J. Herzfeld, Pavan A. Vaswani, Mollie K. Marko, and Reza Shadmehr. A memory of errors in sensorimotor learning. *Science*, 345(6202):1349–1354, 2014.

[45] Ken Takiyama, Masaya Hirashima, and Daichi Nozaki. Prospective errors determine motor learning. *Nature Communications*, 6(1):1–12, 2015.